Monthly Notices of the ROYAL ASTRONOMICAL SOCIETY

MNRAS **517,** 222–239 (2022) https://doi.org/10.1093/mnras/stac2086
Advance Access publication 2022 July 29

Predicting biosignatures for nutrient-limited biospheres

A. E. Nicholson [1]★ S. J. Daines,[2] N. J. Mayne,[1] J. K. Eager-Nash,[1] T. M. Lenton[2] and K. Kohary[1]

[1]*Physics and Astronomy, College of Engineering, Mathematics and Physical Sciences, University of Exeter, Exeter EX4 4QL, UK*
[2]*Geography, College of Life and Environmental Sciences, University of Exeter, Exeter EX4 4QD, UK*

Accepted 2022 July 22. Received 2022 July 14; in original form 2022 March 28

ABSTRACT

With the characterizations of potentially habitable planetary atmospheres on the horizon, the search for biosignatures is set to become a major area of research in the coming decades. To understand the atmospheric characteristics that might indicate alien life, we must understand the abiotic characteristics of a planet and how life interacts with its environment. In the field of biogeochemistry, sophisticated models of life-environment coupled systems demonstrate that many assumptions specific to Earth-based life, e.g. specific ATP maintenance costs, are unnecessary to accurately model a biosphere. We explore a simple model of a single-species microbial biosphere that produces CH_4 as a byproduct of the microbes' energy extraction – known as a type I biosignature. We demonstrate that although significantly changing the biological parameters has a large impact on the biosphere's total population, such changes have only a minimal impact on the strength of the resulting biosignature, while the biosphere is limited by H_2 availability. We extend the model to include more accurate microbial energy harvesting and show that adjusting microbe parameters can lead to a regime change where the biosphere becomes limited by energy availability and no longer fully exploits the available H_2, impacting the strength of the resulting biosignature. We demonstrate that, for a nutrient-limited biosphere, identifying the limiting nutrient, understanding the abiotic processes that control its abundance, and determining the biospheres ability to exploit it, are more fundamental for making type I biosignature predictions than the details of the population dynamics of the biosphere.

Key words: astrobiology – Earth – planets and satellites: atmospheres – planets and satellites: terrestrial planets.

1 INTRODUCTION

With recent instrumentation advances such as the launch of the James Webb Space Telescope and the Extremely Large Telescope (currently under construction), alongside future missions such as the Large Ultraviolet Optical Infrared Surveyor, searching for signs of life on planets beyond our Solar system is set to be possible in the coming decades (Quanz et al. 2021; Snellen et al. 2021). The large diversity of exoplanets found to date indicate that potential biosignatures on different planets will likely manifest in different ways. Any potential biosignature must be understood within the context of its host planet (Seager 2013; Claudi 2017; Kiang et al. 2018; Schwieterman et al. 2018; Krissansen-Totton et al. 2022). One well-known example of how planetary context is important for potential signs of life is the presence of atmospheric oxygen. The presence of oxygen in our atmosphere is a by-product of biological processes and thus would act as a biosignature for remote observers of Earth, however, high O_2 concentrations are possible abiotically for planets under different conditions to our planet (Meadows et al. 2018). Finding and understanding any potential biosignatures will depend on our observational limits (Fujii et al. 2018), our understanding of the abiotic processes at work on the candidate planet (Catling et al. 2018; Krissansen-Totton et al. 2022), and our understanding of how life interacts with its environment (Lovelock & Margulis 1974; Margulis & Lovelock 1974).

Currently, Earth remains our only known example of a life–hosting planet and thus represents the natural starting point for understanding the possibility of detecting life elsewhere. However, Earth's biosphere has evolved significantly during its lifetime to date. Evidence for life on Earth, from the rock record, has now been found essentially at the earliest point possible (e.g. Nisbet & Sleep 2001) during the Archean period. The biosphere at the time was likely the simplest configuration and comprised of methanogens (Schopf et al. 2018). Given that Earth spent roughly a third of its lifetime in the Archean (Catling & Zahnle 2020a), it is natural to begin our study of the vast possibilities for biosignatures with this long–lived and comparatively simple biosphere. In this study, we incorporate well-studied principles from ecology and microbiology into a simple biosphere model, but allow the precise characteristics of our life to be free parameters, exploring the cases that ultimately support a stable population and, a potential, biosignature.

A framework for assessing potential biosignatures has been proposed by Catling et al. (2018) where they suggest a probabilistic approach that combines observations of the candidate planet and its host star with models of the possible abiotic and biotic processes taking place on the planet to determine the probability of the planet being inhabited. Their framework proposes a process roughly following the outline: (1) characterizing the stellar and exoplanetary system properties, including external exoplanet parameters (e.g. mass

★ E-mail: arwen.e.nicholson@gmail.com

and size); (2) characterizing of internal exoplanet properties (e.g. climate); (3) assessing potential biosignatures within the environmental context; and (4) exclusion of false positives. Only by assessing all these details can we make predictions as to whether the presence of a certain feature in a planet's atmosphere is likely due to life or abiotic processes.

This work falls under step (3) of the Catling et al. (2018) process. Understanding a potential biosignature for any particular planet requires models to help us understand what processes we expect to be happening on the planet in the absence of life, and how life would interact with its planet. While determining the potential metabolic pathways for life will be vital when considering possible biosignatures, we will demonstrate that for a simple model biosphere limited by nutrient availability understanding the underlying population dynamics of the biosphere is not necessary to predict the 'strength' of the biosignature produced. Instead, understanding the limiting nutrient is more fundamental and, as we will demonstrate, large differences in the total population of the biosphere only result in small differences in the strength of a biosignature. Population dynamics in this work refers to factors such as the total population of the biosphere, and the rates of death and reproduction, but not to any motion of microbes moving in their environment.

Although this insensitivity of the population dynamics of life to its larger scale impact, and the importance of limiting factors, is well-known across studies of Earth history (Herman & Kump 2005; Kharecha, Kasting & Siefert 2005; Bruggeman & Bolding 2014; Lenton, Daines & Mills 2018; Zakem, Polz & Follows 2020), its implications represent an important shift in our approach to biosignatures. Models of biogeochemistry used to investigate Earth's climatic history, such as the Archean environment (Kharecha et al. 2005) or the rise of oxygen in Earth's atmosphere (Lenton et al. 2018), use sparse data from Earth history to recreate past climates, and much of this research has implications for the search for biosignatures. With our planet as the only known home to life, our assumptions about possible alien life will be biased by the life, both past and present, that we find on Earth. However, if we can minimize the number of assumptions needed to model alien life, and avoid as many Earth-life assumptions as possible, we can formulate robust predictions for how potential biosignatures might manifest on alien worlds. In this work, we take a step towards this goal. Using a simple model, built on fundamental principles of microbial life on Earth, we demonstrate that for a nutrient-limited single-species biosphere the ability of the biosphere to exploit its limiting nutrient is more fundamental to determining the planet's biosignature than the total population. Future work (Daines et al., in preparation) aims to expand on this goal towards a minimal model of biology for more general use in forming biosignature predictions.

A classification of gaseous biosignatures has been proposed by Seager, Bains & Hu (2013a) is as follows: type I biosignatures are generated as a by-product from microbial energy extraction. Type II biosignatures are gases produced as by-products from building biomass, and type III biosignatures are those that are produced by life but not as by-products of their central chemical functions. In this work, we consider type I biosignatures in the above classification scheme and any references to biosignatures in this work will refer to this classification of biosignature unless otherwise stated.

We present a highly simplified model of an Archean-Earth-like planet, home to a single species of life that produces methane as a by-product of energy extraction. On our model planet, there is no abiotic source of methane allowing us to take this gas as a clear biosignature. We demonstrate that, assuming the microbes ability to exploit the limiting resource (in this case H_2) remains unchanged, the details of the population dynamics of the biosphere are largely irrelevant to the abundance of methane in the atmosphere. Instead, we demonstrate that the availability of the limiting resource, in this case hydrogen has a much stronger impact on the abundance of atmospheric methane. In this study, we model the abiotic environment and the microbe behaviour in a highly simplified manner to allow us to determine the relationship between the population dynamics of the biosphere and the resulting biosignature more easily. This study acts a step forward in complexity from more abstract models of life-environment coupled systems (Williams & Lenton 2007; Nicholson et al. 2017, 2018a, b; Alcabes, Olson & Abbot 2020) inspired by realistic models of biogeochemistry designed to recreate ecosystems and climates in Earth history (Herman & Kump 2005; Kharecha et al. 2005; Bruggeman & Bolding 2014; Lenton et al. 2018).

This work takes a step towards the goal of determining the minimal biological assumptions needed to contemplate possible type I biosignatures in scenarios where life is limited by nutrient availability. Future work will certainly be necessary to build on the complexity of the present approach, and enhance the range and precision of the parameters controlling the various processes. Our goal here is just to focus on the simplest problem possible to begin the journey of understanding the key elements of the wider life–planet interaction.

The paper is structured as follows, in Section 2, we detail our simple model set-up for both the planet and the microbes. In Section 3, we outline the specific experiments we have performed, before presenting and discussing our model results in Section 4. Finally, we extend our work to include more realistic process for the amount of energy generated by the microbe's metabolisms in Section 4.5, before concluding in Section 5 and looking forward for future potential steps in Section 6.

2 MODEL SETUP

We simulate a highly simplified zero-dimensional Archean Earth-like planet covered in a global ocean. We keep the model set-up simple in order to develop a tractable framework for exploring the interactions between population dynamics and the atmosphere for a simple methanogen biosphere living in an Archean Earth-like environment.

Life on Earth emerged at least 3.8 billion yr ago (Woese & Fox 1977; Nisbet & Sleep 2001) and methanogens – life that consumes H_2 and CO_2 and excretes CH_4 are thought to be some of the earliest lifeforms (Schopf et al. 2018). We base our model on a planet with newly emerged life before huge diversification occurred. In our model, we consider only a single species of life – single-celled methanogens. We restrict life to the ocean of our planet, and assume that both the ocean and atmosphere are well-mixed. This simplification is justified as we are not modelling the atmosphere or ocean over short time-scales. We explore scenarios where microbe growth is limited by the availability of H_2 to the ocean. We assume the microbe uptake of H_2 is limited only by availability, and so the biosphere is able to fully exhaust H_2 in the ocean. This is a simplification on how nutrient uptake occurs in real microbes (see Section 2.2 for further discussion).

In order to capture the primary mechanisms determining the interaction of life with a planetary climate, we need to describe the cycling of the key chemicals in the system, the response of the planetary climate to changes in composition, and the processes performed by or controlling life (such as cycling of chemical species, population growth, death, etc.), here described as a population of single-celled organisms. In the following sections, we describe how

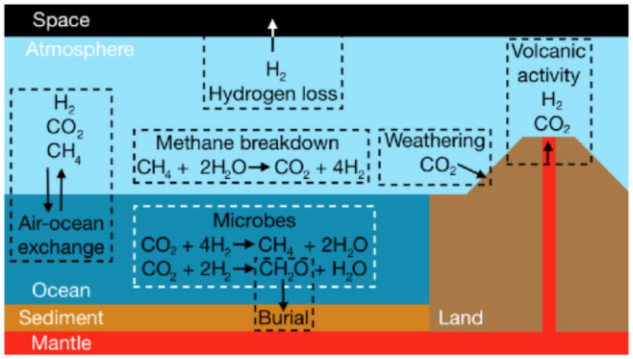

Figure 1. A schematic showing the key abitoic (black-dashed boxes) and biotic (white-dashed box) processes occurring in our model.

we capture each of these key elements as simply as possible. Fig. 1 shows a schematic of our model demonstrating the key processes occurring on the planet. Abiotic processes are shown surrounded by a black-dashed box, and biotic processes by a white-dashed box.

2.1 Planet setup

We track three chemical species in our planet's atmosphere and ocean: H_2, CO_2, and CH_4. The rest of the atmosphere is assumed to be made up of N_2 as this is the most abundant part of Earth's atmosphere. We assume abundant H_2O is available for all chemical reactions requiring it. We also assume the atmospheric pressure (P_{atmo}) and total number of moles of gas in the atmosphere (n_{atmo}) remain constant throughout each experiment, at $P_{atmo} = 1$ atm, and $n_{atmo} = 1.73 \times 10^{20}$ moles, taking modern Earth values. We update the abiotic environment in our model in time-steps representing years.

2.1.1 *Atmospheric* H_2

We assume a source of H_2 via an approximation of out gassing from volcanoes. We also assume a constant rate of removal of H_2 from the atmosphere, although this process is different to the way CO_2 is removed. On Earth, H_2 is irreversibly lost to space via hydrogen diffusion out of the upper layers of our atmosphere. The rate of this loss depends on the mixing ratios of the hydrogen bearing chemical species in the stratosphere (Hunten 1973; Walker 1977). If we assume a dry stratosphere, the rate of hydrogen loss is proportional to $f(H_2) + 2f(CH_4)$ where $f(H_2)$ and $f(CH_4)$ are the mixing ratios of H_2 and CH_4. To keep with the simplified nature of our model, to perform H_2 loss from our model atmosphere we remove a percentage of H_2 proportional to $T(H_2) + 2T(CH_4)$, where $T(H_2)$ and $T(CH_4)$ are the total number of moles of H_2 and CH_4 in the atmosphere.

2.1.2 *Atmospheric* CO_2

We assume a constant source of CO_2 to the planet's atmosphere in an approximation of volcanic out gassing. CO_2 is removed by removing a fixed percentage of the atmospheric CO_2 each year. This is a huge simplification of silicate weathering – a chemical process that removes CO_2 from Earth's atmosphere that is temperature and humidity dependent (Brady & Carroll 1994). During weathering, CO_2 reacts with minerals in surface rocks and is removed from the atmosphere. In our model, we set the abiotic influx and rate of outflux of CO_2 in the atmosphere to be kept constant for the duration of each experiment. As we will be exploring scenarios where H_2 is the limited resource on microbe growth, the details of the H_2 cycle on our planet are more important to microbe metabolic activity than those of the CO_2 cycle allowing us to use a simplified mechanism for CO_2 removal from the atmosphere. In addition, we are not exploring time-scales long enough for impacts of a brightening star to have an effect on the planet's climate.

2.1.3 *Atmospheric* CH_4

In our model, there is no abiotic source of CH_4, however, as we will detail in Section 2.2, our model microbes excrete CH_4 as a by-product of their metabolism. Avoiding any abiotic source of methane makes measuring the hypothetical biosignature on the planet easier as any methane in the atmosphere must be due to biological activity. Additionally, biotic production of methane was much higher than abiotic production during the Archean (Kasting 2005), the period of Earth history our model is loosely based on. Today, CH_4 is rapidly oxidized limiting the build-up of methane in the atmosphere, but in the low O_2 atmosphere of the Archean, O_2 would have rapidly been rapidly consumed and CH_4 was long-lived (Catling, Zahnle & McKay 2001). On real planets, the breakdown of atmospheric methane by photolysis is a complex process that depends on the altitude of the CH_4 and involves several stages. Here, we simplify this and assume that methane breaks down back to CO_2 and H_2 in the atmosphere following

$$CH_4 + 2H_2O \rightarrow CO_2 + 4H_2. \quad (1)$$

This reaction is a combination of the overall methane photolysis pathway of methane at high altitudes, following

$$CH_4 + 2CO_2 \rightarrow 2CO + 4H, \quad (2)$$

and CO removal performed by life via a few metabolisms that combine to form

$$4CO + 2H_2O \rightarrow 3CO_2 + CH_4, \quad (3)$$

following the work of Kharecha et al. (2005). Equations (2) and (3) can then be combined to produce equation (1), our process for CH_4 removal from the atmosphere. Without a process removing CO, it will rapidly build-up in the atmosphere, known as CO runaway (Kasting, Zahnle & Walker 1983; Zahnle 1986), and become an abundant energy resource for life to exploit. We therefore assume a process removing CO from the atmosphere without modelling an additional life form in our model. The experiments presented in this paper will be limited by H_2 availability, not CO_2, and so it is sufficient to say that the carbon cycle is closed without too much concern as to the nature of the process removing CO from the atmosphere. If, however, our experiments were carbon limited, this simplification would break down as the details of the carbon cycle would become more important than those of the hydrogen cycle. The availability of CO to any CO consuming life-form will be dependent on the metabolic waste of methanogens – the life form excreting the CH_4 that in turn is photolysized to produce CO (equation 2). Therefore, methanogens are the primary producers for the ecosystem and their population dynamics will determine the dynamics of lifeforms reliant on their waste products. We assume that equation (1) occurs at a constant slow rate.

These abiotic processes are simplifications of much more complex processes that occur on planets. On a real planet, these processes will change over time and depend on many factors, e.g. changing tectonic activity or involving temperature dependence. As we are interested in

Table 1. Parameters for the influx and outflux of atmospheric CO_2, H_2, and CH_4, where $T(X)$ is the total number of moles of molecule X in the atmosphere.

Chemical	Influx (yr^{-1})	Outflux (yr^{-1})
CO_2	10^{16}	$0.001 \times T(CO_2)$
H_2	10^{14}	$0.001 \times (T(H_2) + 2T(CH_4))$
CH_4	0	$0.001 \times T(CH_4)$

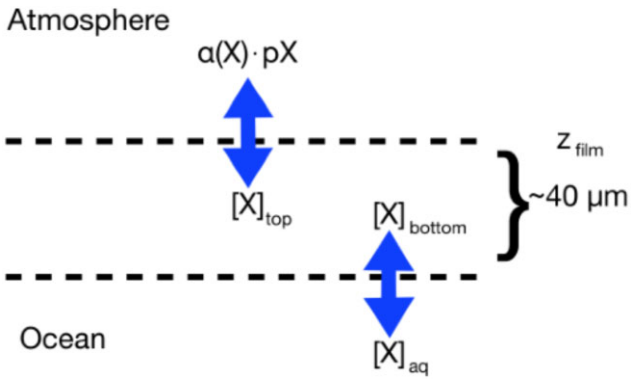

Figure 2. The stagnant layer model for gas exchange between the atmosphere and ocean through a thin film of thickness z_{film}, where $\alpha(X)$ solubility of X (i.e. the Henry's law coefficient), pX the partial pressure of X (in Bar), $[X]_{aq}$ is the dissolved concentration of X (in $mol\,m^{-3}$), and $[X]_{top}$ $[X]_{bottom}$ are the concentrations of X at the top and bottom of the film, respectively.

the overall behaviour of the simple life-environment coupled system and are not trying to recreate the climate of a real planet, we use these simplifications to keep the abiotic environment simple while tracking the abundances of CH_4, CO_2, and H_2.

Table 1 shows the values for the influxes and outfluxes of CO_2, H_2, and CH_4 for our system. These are kept fixed throughout our experiments. For methane, the outflux is the percentage of atmospheric CH_4 that undergoes the process described by equation (1) per year.

2.1.4 *Ocean-atmosphere gas exchange*

The gases in the model atmosphere can dissolve into the global ocean where they become available to life. In another simplification, we assume no other source of H_2 or CO_2 to the ocean except which dissolves into the ocean, and assume no outflux other than out gassing into the atmosphere. We calculate the transfer of gas between the atmosphere and ocean following the stagnant boundary layer model (Liss & Slater 1974). We assume the rate of exchange of gases between the atmosphere and the ocean depends on the concentration gradient of those gasses through a very thin film on the top of the ocean – the stagnant layer. Fig. 2 shows a schematic of this model for how gases are exchanged between the ocean and atmosphere.

The rate of exchange of a chemical between the atmosphere and ocean is set by its relative concentrations

$$\Phi_X = v_p(X) \cdot (\alpha(X) \cdot pX - [X]_{aq}), \tag{4}$$

where Φ_X is the molecular flux of a chemical species X from the atmosphere into the ocean, $v_p(X)$ is the piston velocity of the chemical species X (which can be thought of as the speed at which a gas is being pushed into (or out of) the water column), $\alpha(X)$ solubility of X (i.e. the Henry's law coefficient), pX partial pressure of X (in Bar), and $[X]_{aq}$ is the dissolved concentration of X (in $mol\,m^{-3}$). We calculate the dissolved concentration of H_2, CO_2, and CH_4 in the ocean assuming an ocean depth of 100m. $v_p(X)$ is calculated by dividing the thermal diffusivity of X by the thickness of the film z_{film}, which we assume to be $z_{film} = 40\ \mu m$ (Kharecha et al. 2005). Table 2 shows the values for the parameters needed to calculate the gas exchange between the atmosphere and the ocean for CO_2, H_2, and CH_4.

2.1.5 *Temperature dependence on* CH_4 *and* CO_2

The surface temperature of a planet, in the absence of life, will depend on many properties of the planet and host star. Furthermore, several biotic processes can impact the planetary climate. For our simplified system, we capture the life-climate interaction through a parametrized treatment of the surface temperature as a function of atmospheric composition, generated using an idealized general circulation model. Our model life then changes the planet's atmospheric composition via its metabolic activity (Section 2.2) and in turn impacts the average surface temperature. We use the Met Office Unified Model (UM) – a climate model adapted for exoplanets (Boutle et al. 2017; Eager et al. 2020) to capture 'snapshots' of the planetary temperature for differing atmospheric CO_2 and CH_4 concentrations. Both these important greenhouses gases are thought to have been more abundant in the Archean when life emerged and have provided significant warming (Catling & Zahnle 2020b), so we restrict ourselves to considering the temperature dependence on only these two gases. In this study, we will focus on methane as this is the atmospheric biosignature produced by the microbes on our model planet.

To generate our CO_2, CH_4 and temperature relationship we run a UM simulation set-up as described in Eager-Nash et al., in preparation. This is essentially a version of the Global Atmosphere configuration 7.0 (Walters et al. 2019) adapted to the Archean Earth, with a simplified slab ocean and surface with constant radiative properties. The bulk properties defining a planetary system within the UM – the planet radius, and the properties of the host star, are given in Table 3.

To generate data points for the average surface temperature dependence on atmospheric CO_2 and CH_4, we run a UM configuration for the desired atmospheric composition for 10 yr to reach equilibrium and then run for another 10 yr and average the surface temperature for this time. Within the UM, the atmospheric abundance of a gas is given in terms of the mass mixing ratio – this is the ratio of the mass of the gas in the atmosphere to the total mass of the atmosphere. Fig. 3(a) shows the snapshots of temperature versus CO_2 and CH_4 used in our model, and Fig. 3(b) shows this same data interpolated to create a 2D grid we can then use in our life-climate coupled model. We use this grid to look up the corresponding average surface temperature for any atmospheric composition throughout our experiments.

2.2 Microbe setup

We restrict life to a single species of single-celled methanogens that generate adenosine triphosphate (ATP), an organic compound that provides energy for cellular processes, via the following metabolism

$$CO_2 + 4H_2 \rightarrow CH_4 + 2H_2O, \tag{5}$$

and creates biomass from

$$CO_2 + 2H_2(+ATP) \rightarrow CH_2O + H_2O. \tag{6}$$

We explore two scenarios for the energy obtained from the microbes' metabolism, equation (5); the first, labelled energy scheme

Table 2. Parameters for the atmosphere-ocean exchange of CO_2, H_2, and CH_4. $*$: CH_4 and H_2 values from Kharecha et al. (2005), α: CO_2 diffusivity value from Zhang et al. (2018), β: CO_2 solubility from https://webbook.nist.gov/chemistry/. Piston velocities are calculated assuming a stagnant boundary layer thickness of $z_{film} = 40\ \mu m$. We assume 25°C for the values for our gases and keep this fixed.

Chemical	Piston velocity ($m\,s^{-1}$)	Diffusivity ($m^2 s^{-1}$)	Solubility $mol\,L^{-1} bar^{-1}$
CO_2	6.7×10^{-4}	$2.67 \times 10^{-6}\ ^{\alpha}$	$0.035\ ^{\beta}$
H_2	$1.3 \times 10^{-2}\ *$	$5.0 \times 10^{-5}\ *$	$7.8 \times 10^{-4}\ *$
CH_4	$4.5 \times 10^{-3}\ *$	$1.8 \times 10^{-5}\ *$	$1.4 \times 10^{-3}\ *$

Table 3. Bulk parameters for the zero-dimensional Archean Earth-like model planet.

Parameter	Value
Planet radius	$6051.3 \times 10^3 m$
Star spectral class	G-type main sequence
Star age	1 billion yr

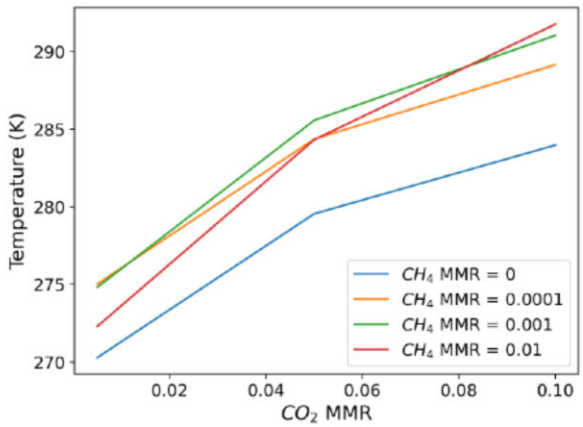

(a) 'Snapshots' obtained from the Unified Model.

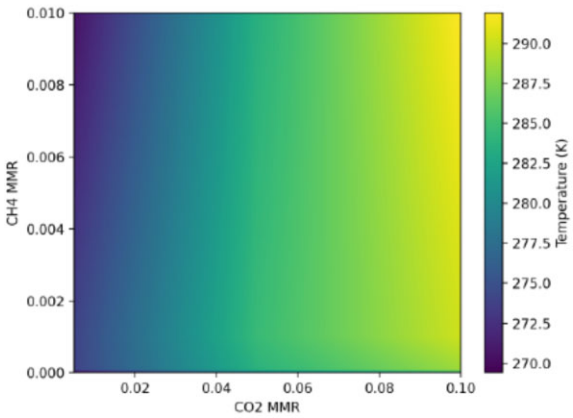

(b) Interpolated data.

Figure 3. Global average surface temperature dependence on atmospheric levels of CH_4 and CO_2 mass mixing ratios.

(a), where there is a fixed energy yield for metabolizing 1 mole of H_2 representing a simplified case. This approach is typical in abstract models of life-environment coupled systems (e.g. Williams & Lenton 2007; Nicholson et al. 2018b).

We then explore a second scenario, labelled energy scheme (b), where the energy yield from metabolizing is determined by the free energy form of the Nernst equation following Kharecha et al. (2005), described by

$$\Delta G = \Delta G^0 + R\ T\ log(Q) \tag{7}$$

where ΔG^0 free energy change of the reaction under standard conditions (i.e. unit concentrations of the reactants and products), R = universal gas constant $=0.008314 kJ\,mol^{-1}\,K^{-1}$, and $T = 298\ K$ (the assumed water column temperature). Q is calculated using

$$Q = \frac{[CH_4]^*_{aq} \cdot a(H_2O)^2}{[CO_2]^*_{aq} \cdot ([H_2]^*_{aq})^4}, \tag{8}$$

where $[i]^*_{aq} = \frac{[i]_{aq}}{\alpha(i)}$ – the dissolved concentration of species i divided by its Henry's law coefficient, and $a(H_2O)$ is assumed to be 1 (Kharecha et al. 2005). Following Kral et al. (1998), we assume that $\Delta G^0 = (-253 + 0.41\ T) kJ\,mol^{-1}$. We explore these two energetic scenarios to allow us to observe how the behaviour of our model changes with incremental increases to its complexity.

For the experiments presented in this study, there are no restrictions on the growth of methanogens other than the availability of CO_2 and H_2. We assume that microbes can uptake H_2 at a maximum rate of $C^{H_2}_{max}$ (see Table 4), and no set minimum rate as long as there is H_2 in the ocean for the microbes to consume. Studies of microbes on Earth show that metabolic rates vary in response to the environment (e.g. competition for resources etc.) up to some maximum value based on studies of microbes in 'ideal' laboratory conditions (Brown et al. 2004; Monod 2012; Li et al. 2019). In our model, this fundamental principle is accounted for through the variation in H_2 uptake to a maximum rate. This approach follows the abstract representations of life used in abstract life-environment coupled models (e.g. Williams & Lenton 2007; Nicholson et al. 2018b). This means that in this model the microbes can draw the concentration of H_2 in the ocean down to zero. Real microbes are limited by diffusion of H_2 (and other required nutrients) across their cell membranes, and microbes have evolved a range of adaptations to maximize the rate of diffusion into their cell, from changing cell sizes and shapes, to growing filaments to maximize surface area, and developing strategies to move to areas of higher resource concentration (Beveridge 1988; Koch 1996; Siefert't & Fox 1998; Schulz & Jørgensen 2001; Young 2006). Therefore, real methanogens cannot draw H_2 concentrations to zero as they require a chemical gradient between themselves and their environment in order to uptake nutrients. We make the assumption in this study that the microbes have evolved to exploit H_2 to the same limit for every experiment presented, and for simplicity, we take this

Table 4. Model methanogen parameter values. $*$ from Lynch et al. (2019), α from Janssen et al. (1996).

Parameter	Value
Maintenance ATP cost per microbe	$2.16 \times 10^{-19} mol_{ATP}\ cell^{-1} s^{-1}$ *
Growth ATP cost to build one microbe	$4.23 \times 10^{-14} mol_{ATP}\ cell^{-1}$ *
Maximum rate of H_2 consumption per microbe – $C^{H_2}_{max}$	$3.76 \times 10^{-17}\ mol_{H_2} cell^{-1} s^{-1}$ *
Microbe cell protein (CH_2O) content	$7.4 \times 10^{-15}\ mol_{CH_2O}\ cell^{-1}$ *, α
Death rate of microbe population	1 per cent of population per hour
Energy scheme (a) – moles of ATP obtained per mole of H_2 consumed	$0.15\ mol_{ATP}\ mol^{-1}_{H_2}$ *
Energy scheme (b) – energy required to form 1 mole of ATP	$32.5 kJ\ mol^{-1}_{ATP}$ *

limit to be zero. In this study, we are interested in comparing different population dynamics of biospheres that otherwise interact with the abiotic environment in the same way, e.g. the same metabolic pathways and the same ability to exploit limiting nutrients. This allows us to isolate any dependence of the resulting biosignature on these population dynamics in a simple manner. For accurate predictions of biosigatures for real planets, understanding the limit to which a resource, in this case H_2, can be exploited by life will be important.

As we only explore scenarios where H_2 availability is the limiting factor on microbe growth as CO_2 is far more abundant than H_2 on the model planet, the uptake of CO_2 by the microbes is determined by the uptake of H_2. Therefore, if microbes are consuming H_2 to generate biomass they will consume 1 mole of CO_2 for every 4 moles of H_2 following equation (5). If the microbes are instead generating ATP they will consume 1 mole of CO_2 for every 2 moles of H_2 following equation (6). If instead we modelled scenarios, where CO_2 was more scarce than H_2, then the uptake of H_2 would depend on the uptake of CO_2 instead.

Another simplification made in our model is that when the microbes die, their bodies are buried with 100 per cent efficiency, i.e. no recycling takes place. This means that once a microbe dies, the CH_2O that makes up its cell is removed from the system. This simplification allows us to avoid introducing additional chemical reactions for the breakdown of CH_2O (although incorporating more complex ecosystems is something we plan to explore in future work). There are two ways microbes can die in our model – (1) starvation due to insufficient ATP for maintenance and (2) via a constant death rate that represents death from any other cause. This background death rate effectively sets an average lifespan for the microbes.

The model microbes impact their planet via their metabolism and biomass creation. They remove H_2 and CO_2 from the ocean and excrete CH_4. Due to the exchange of gases between the atmosphere and the ocean (equation 4) this then impacts the surface temperature of the planet (as detailed in Section 2.1.5).

Table 4 shows the default parameter values used for our model microbes. These values for the microbe cell maintenance, ATP cost for maintenance and cell growth, maximum uptake of H_2 per cell ($C^{H_2}_{max}$), and ATP generated via their metabolism, are used for our initial experiments and then these values are changed to measure the sensitivity of our model results on these parameters.

The protein (CH_2O) content of a cell is calculated assuming that $m_{cell} \approx 2\, m_{cell\,protein} = 4.44 \times 10^{-13} g$ (Janssen et al. 1996; Lynch et al. 2019). As another simplification microbes starve instantly if they do not have sufficient ATP for maintenance within the current time-step (although in reality it can take microbes far longer to die from starvation; dormancy is as a common strategy for microbes living under resource limitation, Lennon & Jones 2011).

A standard method to model populations of life is through agent-based dynamics, where we simulate the actions of individual agents to understand the behaviour of a system, and this approach is often used in ecological models (Christensen et al. 2002; Grimm & Railsback 2013; Nicholson et al. 2018b). However, as our populations grow large, this approach is not computationally feasible. Therefore, as we are aiming to capture the bulk population properties, we consider the population in terms of the total ATP contained within it. In some abstract models of life-environment coupled systems, such as the Flask model (Williams & Lenton 2007) or the ExoGaia model (Nicholson et al. 2018b), microbes within the model accumulate biomass over the course of the experiment and they must 'spend' a certain amount of biomass each time-step in an maintenance cost. Additionally, there are biomass thresholds for starvation and reproduction where microbes die when their biomass drops below the 'starvation threshold', and reproduce when their biomass exceeds the 'reproduction threshold'. For real, microbes maintenance costs (the energy required by a microbe for processes other than biomass generation) are given in terms of ATP (Şengör et al. 2013; Lynch et al. 2019). Therefore, as we can consider microbe growth in terms of the biomass created per mole of ATP (Şengör et al. 2013); instead of tracking the biomass within our population, we track the ATP contained within the population and assume a constant amount of biomass per microbe (see Table 4). Therefore, in our model, a microbe will accumulate ATP, using some for maintenance as needed, until it accumulates enough ATP to generate sufficient biomass for a new microbe, at which point it reproduces. Therefore, to track the population dynamics of the microbes, we require a calculation of the total ATP within the population, alongside that lost due to starvation and 'spent' during maintenance and reproduction. Our treatment of these elements is described in the following sections.

2.2.1 *Distribution of ATP in population*

Biomass within microbe cells varies even within the same species (Cermak et al. 2017) and a normal distribution has been used to capture diversity in agent-based models of microbes (Hellweger & Bucci 2009). We consider our microbe population in terms of ATP contained within the population and represent this as a normal distribution centred around μ_s – the mean ATP available to a cell, and with variance of $\sigma_s = 0.1\mu_s$, an approach used in Nicholson et al. (2017, 2018a, b). Therefore, for our microbe population, the number of microbes containing x moles of ATP, $f_s(x)$, is given by

$$f_s(x) = \frac{p_{tot}}{\sigma_s\sqrt{2\pi}} e^{-\frac{1}{2}\left(\frac{x-\mu_s}{\sigma_s}\right)^2}. \quad (9)$$

where p_{tot} is the total population of the biosphere at the start of the biological time-step. We can then use this distribution to calculate the number of microbes above or below certain thresholds, e.g. the number of microbes with sufficient ATP to reproduce.

2.2.2 Number to starve

Each time-step microbes must 'spend' a certain amount of ATP to maintain basic function, those with insufficient ATP starve to death. To determine the number of microbes that are below this threshold and thus die via starvation, $s_s(a_m)$, we use the cumulative distribution function to determine the population with ATP levels lower than maintenance threshold a_m

$$s_s(a_m) = p_{tot} \int_{-\infty}^{a_m} f_s(x)\, \partial x = \frac{p_{tot}}{2}\left[1 + erf\left(\frac{a_m - \mu}{\sigma\sqrt{2}}\right)\right]. \quad (10)$$

2.2.3 Amount of ATP within starved population

We also need to calculate the amount of ATP contained within microbes that are below the starvation threshold (a_m). This quantity of ATP, $h_s(a_m)$, is given by

$$h_s(a_m) = p_{tot} \int_{-\infty}^{a_m} x f_s(x)\, \partial x = p_{tot} \int_{-\infty}^{a_m} \frac{x}{\sigma\sqrt{2\pi}} e^{-\frac{1}{2}\left(\frac{x-\mu}{\sigma}\right)^2} \partial x. \quad (11)$$

To solve, we substitute

$$\lambda = \frac{x-\mu}{\sigma}, \quad \frac{\partial\lambda}{\partial x} = \frac{1}{\sigma}, \quad c = \frac{a_m - \mu}{\sigma}, \quad (12)$$

to get

$$h_s(a_m) = -\, p_{tot} \frac{\sigma}{\sqrt{2\pi}} e^{-\frac{1}{2}c^2} + p_{tot}\, \frac{\mu}{2}\left(1 + erf\left(\frac{c}{\sqrt{2}}\right)\right). \quad (13)$$

2.2.4 ATP maintenance cost

Once the microbes that die from starvation are removed from the population, the total ATP used for maintenance, m_s, used by the remaining population, r_s, assuming a maintenance cost per microbe of a_m, is given by

$$m_s = r_s \times a_m. \quad (14)$$

2.2.5 Number of microbes to reproduce

Finally, microbes with sufficient ATP to reproduce a_r will do so asexually by splitting into two identical individuals. The number of microbes with sufficient ATP to reproduce $r_s(a_r)$ is calculated by

$$r_s(a_r) = p_{tot} - \frac{p_{tot}}{2}\left[1 + erf\left(\frac{a_r - \mu}{\sigma\sqrt{2}}\right)\right]. \quad (15)$$

3 EXPERIMENT SETUP

In the following section we will present results for a number of experiments. In our model we step forwards in time solving the equations governing the system described previously. We employ two different time-steps, one for biological processes such as microbe death and reproduction, and another for abiotic processes such as H_2 input to the atmosphere. We set the biological time-scale to be an hour, and the abiotic red time-step to be a year. Microbial growth is often measured in units of an hour (e.g. Weissman, Hou & Fuhrman 2021) and so we choose this for the biological time-scale. The climate in the UM simulation set-up (Eager-Nash et al., in preparation) used to determine the relationship between atmospheric composition and surface temperature for this model tends to stabilize over the order of years to tens of years (depending on the starting configuration), and so we choose a year for our abiotic time-scale in our model. For each experiment, we first run the model without life until the ocean and atmospheric chemistry is in equilibrium that takes around ≈12 000 yr (here and throughout 'years' refers to Earth years). Equilibrium is determined when the surface temperature of the planet stabilizes to a constant. We then reset our time counter to zero and introduce life at $t = 20\,000$ yr. Once life is introduced, we run the simulation for a further 40 000 yr after which we then force a total extinction of the biosphere to demonstrate how the planet surface chemistry reacts to the removal of life.

To compare results from different experiments, instead of artificially removing life during the experiment, we instead let the biosphere persist (if the microbes can survive their environment) until the end of the experiment. We then average the last 5000 yr of each experiment to investigate how changing various biological parameters, such as the microbes' death rate or ATP maintenance cost, impacts the resulting biosignature – the abundance of methane in the atmosphere.

Time in the model progresses in terms of hours and years in the following steps:

(i) Update yearly:

(1) Abiotic influx and outflux of H_2, CO_2, and CH_4.
(2) Planetary temperature determined from atmospheric chemical makeup.

(ii) Update hourly:

(1) Exchange of gases between the atmosphere and ocean (equation 4).
(2) Calculate number of microbes that die.
(3) Calculate remaining microbes' ATP maintenance cost.
(4) Calculate number of microbes with sufficient ATP reproduce given sufficient H_2 and CO_2 availability.
(5) Microbes consume remaining H_2 and CO_2 uptake capacity to create ATP and excrete CH_4.

When referring to changing parameters in some of the results presented in this paper, the default values for these parameters are those given in Tables 1 and 4. For each experiment, a seed population size $p_{seed} = 10^2$ is used unless otherwise specified. However, it is demonstrated in Section 4.1 that the model results are insensitive to the size of the seed population used.

In Section 4, we will explore scenarios where H_2 is the limiting resource on microbe growth. We use H_2 as our limiting resource as this mimics the scenarios for life on early Earth. Exploring scenarios for an H_2-dominated atmosphere would also involve including the greenhouse effect of abundant atmospheric H_2 (Pierrehumbert & Gaidos 2011). Instead, we take H_2 as the limiting resource and calculate the average surface temperature based only on the atmospheric content of CO_2 and CH_4. This set-up also means that the starting temperature of all our experiments is the same, even when changing the abundance of the limiting resource that makes for easier comparisons.

The results presented in Section 4 show that life has a significant impact on the methane content of the atmosphere and thus the average surface temperature of its host planet. By excreting CH_4, the microbes raise the average surface temperature of their planet by roughly 5 degrees (K). We will demonstrate that for a simple H_2 limited biosphere significantly changing the microbe parameters,

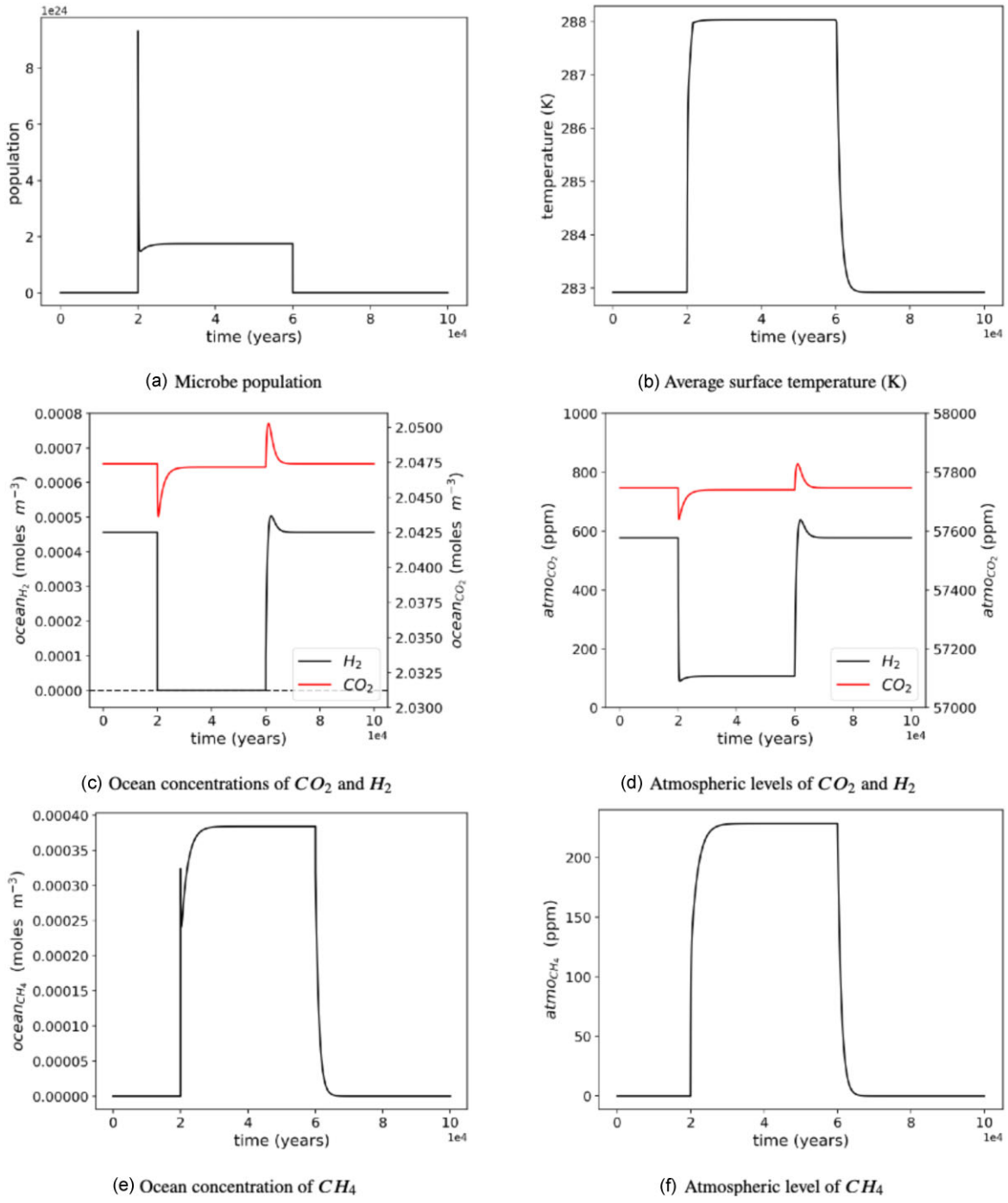

Figure 4. Model results for a single experiment showing how the planet's surface temperature, and the ocean and atmospheric levels of H_2, CO_2, and CH_4 change with the introduction of life at $t = 20\,000$. The dashed line in panel (c) shows a concentration of zero of H_2 dissolved in the ocean.

such as microbe death rate or maintenance ATP cost, does not significantly change the CH_4 level in the atmosphere due to the biosphere. Although the microbe population can change significantly when changing biological parameters, the resulting change in the total CH_4 output by the biosphere is much smaller. Changing the influx of H_2 to the system, however, has a much stronger impact on the level of CH_4 in the atmosphere as the increased availability of H_2 supports a higher population of microbes that in turn increases the total CH_4 output of the biosphere.

4 MODEL RESULTS

Here, we first present the results from a single experiment with parameters set to the default values found in Tables 1 and 4 in Section 2.2. Initially the planet is devoid of life and at $t = 20\,000$ yr we seed the planet's ocean with our model microbial life. We then run the simulations with life for a further 40 000 yr, and then impose a total extinction at 60 000 yr, removing all life.

Fig. 4 shows the output of a single run of our model. Fig. 4(a) shows the microbe population over time, and 4(b) shows the average

surface temperature of the planet. Figs 4(c and e) show the abundance of CO_2, H_2, and CH_4 and in the ocean and Figs 4(d and f) show these abundances for the atmosphere. The impact of the appearance of life on the planet is immediately apparent in all six panels of Fig. 4. Fig. 4 also shows that when life is removed from the planet that the atmospheric and ocean chemistry rapidly, in geological time-scales, return to their previous states after roughly 5000 yr. Therefore, in this model, any biosignature produced by life is short lived if life goes extinct.

Fig. 4(a) shows that the microbe population experiences an initial spike before dropping to a stable population soon after life emerges. This initial spike in the total population is due to microbes emerging on a planet with abundant hydrogen dissolved in the ocean built up over time. Initially microbes are able to consume hydrogen at their maximum rate $C_{H_2}^{max}$ and this leads to exponential growth and a population explosion. As the population grows the biosphere draws down the level of H_2 in the ocean until they exhaust the available H_2. At this point the total population the planet can support is constrained by the influx of H_2 to the system (in this model provided by a representation of volcanic activity). As this is less than the concentration of H_2 that had built up in the ocean before life was introduced, the population rapidly declines until a stable state is reached where the reproduction rate of the microbes matches the death rate. The establishment and maintenance of this stable state once life is introduced to the planet is explored further in Section 4.1.

Figs 4(c and e) shows a rapid transition in the ocean abundances of H_2, CO_2, and CH_4 after life appears on the planet. The ocean concentrations of H_2 and CO_2 are rapidly drawn down as life consumes these chemicals to generate biomass and ATP and CH_4 rapidly accumulates in the ocean as microbes excrete this gas as a byproduct of their metabolism (equation 5). We see that after the initial reduction in the ocean concentration of CO_2, CO_2 in the ocean rises again and stabilizes to a level slightly below the initial concentration. This rise in the concentration of CO_2 in the ocean shortly after the drop corresponding to introduction of life is due to methane breakdown taking place in the atmosphere. Methane is recycled back to CO_2 and H_2 via equation (1) and so this in effect adds an extra input of CO_2 to the atmosphere on top of the influx from volcanic activity. We see in Fig. 4(c) that after the introduction of life, the H_2 concentration in the ocean remains at zero while life persists on the model planet. The asymmetry between the behaviour of ocean levels of CO_2 and H_2 is due to the differences between the removal of H_2 and CO_2 from the atmosphere, see Table 1. Whereas the rate of CO_2 removal in our model depends only on the abundance of CO_2 in the atmosphere, H_2 loss depends on both the abundance of H_2 and CH_4 in an approximation of the process of H_2 loss to space on real planets. As the level of H_2 in the atmosphere decreases, the level of CH_4 rises, and so the loss of H_2 happens at a faster rate than if it were just dependent on atmospheric H_2. The availability of H_2 sets the total population that the planet can support and so in our model the microbes reproduce until H_2 is depleted in the ocean down to a concentration of zero. If CO_2 was instead the limiting resource in our model, the ocean concentration of CO_2 would instead be drawn down to zero.

The behaviour of the abundance of CH_4, CO_2, and H_2 in the atmosphere largely follows what we see in the ocean. After life emerges H_2 and CO_2 are drawn down, levels of CH_4 rise, and we see a rise in atmospheric CO_2, after the initial drop, due to the recycling of methane. A much smaller rise is seen in the level of atmospheric H_2 because of the different process of H_2 removal. We see in Fig. 4(b) that the emergence of life leads to a rapid 5° increase in the temperature of the planet due to the methane building up in the atmosphere as a byproduct of the microbes' metabolism.

4.1 Equilibrium state

The maximum growth rate of the model microbes is set by $C_{max}^{H_2}$ – the maximum rate at which the microbes can uptake H_2. The value for $C_{max}^{H_2}$ in Table 4 is based on studies of microbes in 'ideal' laboratory conditions, in the absence of resource limitation or competition (Monod 2012; Wang et al. 2016; Li et al. 2019; Lynch et al. 2019). $C_{max}^{H_2}$ represents the maximum metabolic rate for a microbe. However, in realistic scenarios, the metabolic rate of microbes changes due to environmental conditions such as resource shortages (Brown et al. 2004). In our model, $C_{max}^{H_2}$ sets the maximum metabolic rate of the microbes, however, their metabolic rate can vary depending on nutrient availability. For a high metabolic rate where the birth rate of microbes exceeds the death rate, population growth will occur, and if their metabolic rate drops such that the growth rate is less than the death rate the microbe population will shrink and if the low growth rate persists total extinction will occur. A stable population is achieved when the growth rate of the microbes is equal to the death rate.

The population at which the biosphere stabilizes at is determined by a feedback loop between H_2 availability per microbe, and microbe growth rate. Initially, when microbes are seeded on to a model planet initially there will be abundant H_2 and microbes will uptake H_2 at their maximum rate – $C_{max}^{H_2}$ (see Table 4). Microbes will be able to quickly accumulate ATP via equation (5) and exponential growth of microbes will occur. This causes the large spike in microbe population soon after seeding seen in Fig. 4(a). As the microbe population grows, the H_2 concentration in the ocean will fall (Fig. 4c).

A point will be reached where the initial rapid growth of the microbes can no longer be supported by the diminishing H_2 content of the ocean, and the growth of microbes will become limited by the inflow of H_2 to the ocean from the atmosphere. This H_2 inflow rate is significantly smaller than the reserves of H_2 that had dissolved into the ocean before the emergence of life and so the high microbe population resulting from the initial exponential growth cannot be supported by the model planet long term. This causes the microbe population to drop. The microbe population will stabilize where the growth rate of the microbes is equal to the death rate of the microbes (Table 4). The growth rate of a microbe depends on the availability of H_2, the ATP maintenance cost of the microbe and the cost of biomass production. If the availability of hydrogen increases, then the metabolic activity of the microbes can increase leading to an increase in the microbes' growth rate and so an increase in the total microbe population. An increase in the total population, however, will decrease the availability of hydrogen per microbe and so the feedback loop is stabilizing. This feedback loop is shown in Fig. 5.

The microbe population will stabilize at a level where, on average, the H_2 availability per microbe is sufficient for that microbe to reproduce once before its death. In this way, a stable population emerges in our model.

The model results are insensitive to the size of the seed population. The initial spike in total population seen upon life emerging on a planet will vary minimally depending on the seed population, but as the stable population is determined by the inflow of H_2 to the ocean, which itself is determined by the influx of H_2 to the atmosphere, the stable population size reached is unaffected by the seed population size, see Fig. 6.

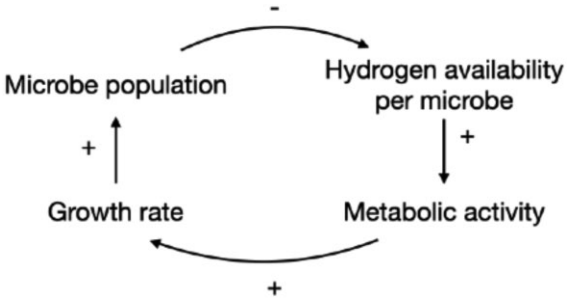

Figure 5. Diagram showing the feedback loop between H_2 availability per microbe, microbe metabolic rate, microbe growth rate, and total microbe population. A + sign indicates that an increase in the source leads to an increase in the sink. A − sign indicates that an increase in the source leads to a decrease in the sink.

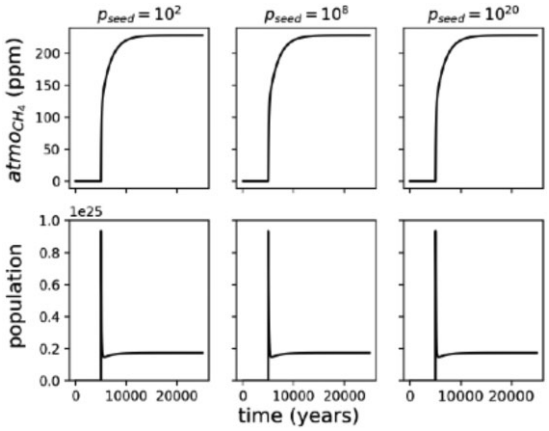

Figure 6. Figures showing the insensitivity of the total population, and the level of CH_4 in the atmosphere ($atmo_{CH_4}$), to the size of the microbial seed population p_{seed}.

4.2 Parameter sensitivity

The parameters used in the model so far are taken from the values found in Table 4, which are based on measurements of methanogens grown in lab settings. However, methanogens on Earth are highly diverse with different variants having different growth rates (Lyu et al. 2018). Therefore, the parameters in Table 4 could clearly be very different for alien life on another planet as they differ significantly between microbes species on Earth. To investigate the sensitivity of our model results to different microbe parameters, we changed the death rate (the percentage of microbes removed from the ocean per hour), microbe cell protein content, and the ATP maintenance cost per microbe, and repeated the experiment. These experiments reveal that the impact of microbes on the wider planetary system is only weakly dependent on these underlying characteristics of the microbes, while a viable biosphere is possible on the planet under the biological parameters chosen for the experiment.

4.2.1 Changing the death rate

We define the death rate as the percentage of microbes that are removed per hour. In our model as there is no breakdown of CH_2O – the building block for our life – microbe bodies are assumed to be removed from the system once dead. We find that while significantly changing the death rate leads to a large change in the total microbe

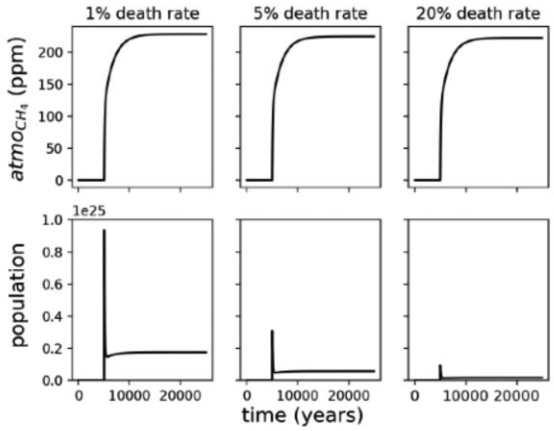

(a) Impact of changing death rate on the atmospheric methane content ($atmo_{CH_4}$) and microbe population.

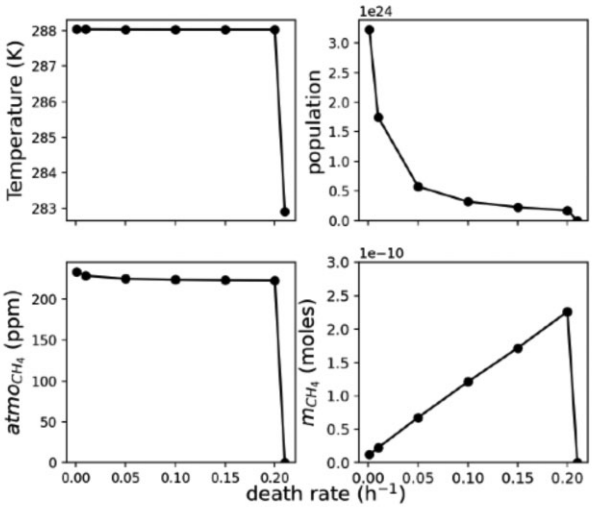

(b) Sensitivity of the surface temperature, microbe population, atmospheric CH_4 content ($atmo_{CH_4}$), and the average CH_4 output per microbe (m_{CH_4}) to changing microbe death rate.

Figure 7. Panels showing the model sensitivity to changing the death rate of the microbes (determined as the fraction of the population removed per hour).

population, it leads to only a small change in the abundance of methane in the atmosphere.

Fig. 7 shows in panel (a) the level of methane in the atmosphere and microbe population over time for differing death rates, and in panel (b) the surface temperature, microbe population, atmospheric CH_4 content, labelled $atmo_{CH_4}$, and the average CH_4 output per microbe per year, labelled as m_{CH_4}, for varying death rates. We explored a range of death rates from 0.1 per cent up to 15 per cent of the population removed every hour. In Fig. 7(b), we show the death rate as the fraction of the population removed per hour instead of the percentage. We see in Fig. 7 that a death rate of over 20 per cent leads to extinction on the planet and no biosignature.

Fig. 7(a) demonstrates how the scale of the impact on the microbe population, and the impact on the abundance of atmospheric methane, differ significantly when adjusting the death rate. Fig. 7(a) shows a clear impact on the microbe population as we change the death rate, as the death rate increases the population decreases. As more microbes are being removed regularly at a higher death rates, this shows an unsurprising result. The impact on the methane in the atmosphere,

however, is far more subtle. A large change in the population leads to only a small change in the abundance of atmospheric methane. Therefore, changing the population dynamics significantly does not lead to a significant impact on the resulting biosignature.

Fig. 7(b) demonstrates the impact on the level of methane in the atmosphere from changing the death rate more clearly and shows that increasing the death rate leads to a small non-linear decrease in atmospheric methane. Due to the non-linear relationship between methane in the atmosphere and surface temperature, we find that the temperature of the planet does not change significantly between each experiment. When we examine the average amount of methane output per microbe per hour – m_{CH_4} – we see why a large change in the population translates to only a small change in the level of atmospheric methane, as we increase the death rate, m_{CH_4} increases. For a higher death rate, the metabolic activity of the average microbe must occur at a faster rate to maintain a stable population. If microbes are being removed from the ocean at a higher rate then the reproduction rate of the microbes must increase to counteract it; this requires microbes to generate ATP faster and therefore increases the CH_4 output per microbe, as methane is a byproduct of the microbes' metabolisms. Therefore, a lower population results in a similar atmospheric methane level as each individual microbe is now outputting CH_4 at a faster rate.

As the maximum rate of H_2 uptake, $C^{H_2}_{max}$, is kept constant for all experiments, a point is reached where, with increasing death rate, it is no longer possible for the microbes to accumulate sufficient ATP to reproduce before they are killed off. Past this point a stable population is not possible and the biosphere rapidly goes extinct.

4.2.2 *Changing additional biological parameters*

We also investigated changing the ATP maintenance cost of the microbes, and their cell protein content (number of moles of CH_2O per microbe) and found that, similar to changing the death rate, these parameters had only a small impact on the abundance of methane in the atmosphere, despite having large impacts on the total population, up until the point where the biosphere collapses due to an insufficient $C^{H_2}_{max}$ for microbe growth.

Fig. 8 shows how the surface temperature, microbe population, level of methane in the atmosphere, and the average methane output per microbe m_{CH_4} change with varying the ATP maintenance cost of the microbes. This is the ATP microbes must 'spend' per second (measured in seconds as this is typical for laboratory measurements of microbes) to maintain basic functions and avoid death via 'starvation' (this is separate from the imposed death rate explored in Section 4.2.1). We explored a range of maintenance costs from 0.01 times the value in Table 4 up to 10 times this value. In our experiments, any microbe with insufficient ATP for this maintenance cost dies immediately and is removed from the system. All other microbe parameters in these experiments, including the death rate, were set to the values found in Table 4.

We find that increasing the ATP cost corresponds with no measurable change to the surface temperature of the planet, a slight increase in the atmospheric level of CH_4, a significant decrease in the microbe population, and again an increase in the value of m_{CH_4} – the average methane output per microbe per year. Increasing the ATP cost per microbe requires the microbes' metabolic rate to increase in order to generate sufficient ATP to maintain a stable population. With microbes 'spending' more of their H_2 and CO_2 intake on ATP production, there is less available for biomass production and so the total population the planet can support is reduced. The increased

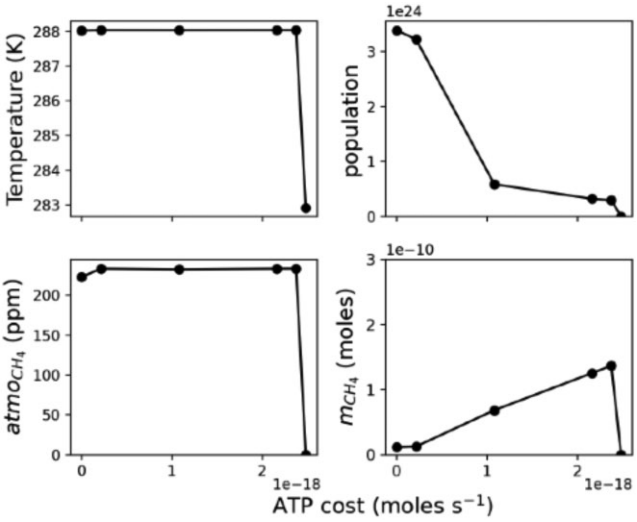

Figure 8. Panels showing the sensitivity of the surface temperature, microbe population, atmospheric CH_4 content ($atmo_{CH_4}$), and the average CH_4 output per microbe (m_{CH_4}) to changing the microbe ATP maintenance cost.

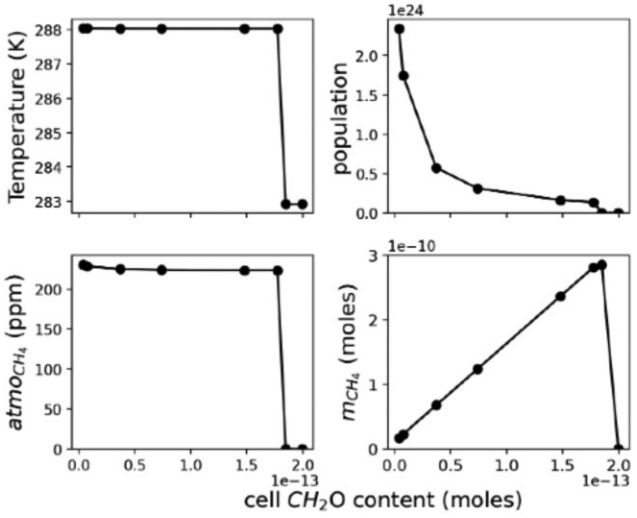

Figure 9. Panels showing the sensitivity of the surface temperature, microbe population, atmospheric CH_4 content ($atmo_{CH_4}$), and the average CH_4 output per microbe (m_{CH_4}) to changing the CH_2O microbe cell content. Note that the ATP required to create a new cell scales linearly with cell CH_2O content.

metabolic activity means that despite the reduced microbe population the amount of methane in the atmosphere rises only slightly with increasing ATP cost.

Fig. 9 shows how the surface temperature, the microbe population, the atmospheric level of CH_4, and the average methane output per microbe per year (m_{CH_4}) change with varying the protein (CH_2O) content of the microbe's cells. As the cell size increases, we increased the ATP 'cost' to form a cell linearly. We varied the CH_2O content of the cell from half of the value in Table 4 to over 25 times this value. We find again a point at which the cell size becomes too large and total extinction occurs as microbes were unable to consume sufficient H_2 and CO_2 to fulfill both their metabolic needs and generate biomass. The second to last data point in Fig. 9 shows a scenario where there is signature of life on the planet, but life has not fully gone extinct. In this case, the total population of the planet was around 6.5

individuals due to the limitations in representing small populations in code designed for populations of the order of 10^{24}. In this case, the microbes at such small numbers have no measurable impact on their planet and such a scenario could represent the remnants of a collapsed biosphere 'clinging on' in small pockets on its planet (Wilkinson 2007). In these experiments, we again set the other microbe parameters to the values in Table 4.

Again, we found that increasing the protein content also only had a slight impact on the level of methane in the atmosphere, while the planet supported a thriving biosphere. As we increased the CH_2O content of a microbe cell, we found again no measurable change in the temperature of the planet, a significant reduction in the total population for increasing cell protein content, a small reduction in the level of atmospheric methane, and an increase in the average methane output per microbe per hour. These results again show that significantly changing the parameters detailing the population dynamics of the simple biosphere only has a small impact on the level of atmospheric methane resulting from the biospheres' metabolic activity, for biological parameters that allow for a successful biosphere. Thus the underlying population dynamics of the biosphere do not significantly impact the resulting biosignature we would expect to measure for our H_2 limited biosphere.

4.3 Burial rate

We can combine the data from our biological experiments if instead of measuring the biosphere in terms of microbe population, ATP generation or death rate, we measure the biological burial rate of H_2. When the microbes die, we assume that the dead cells fall to the bottom of the ocean and are buried, and therefore hydrogen is removed via this process as the microbes cells are built from CH_2O. The burial rate depends on the population of the microbes, the protein content of their cells, and the rate at which microbes are removed from the system. We consider here the burial of rate H_2 as our biosphere is H_2 limited. If carbon dioxide instead was the limiting factor on microbe growth, the burial rates of carbon and oxygen would be more important processes to study.

Fig. 10 shows the relationship between H_2 burial rate and level of methane in the atmosphere in the top panel, and the concentration of H_2 in the ocean in the bottom panel for all of the data presented thus far from our experiments in Sections 4.2.1 and 4.2.2. We find a negative linear relationship between burial rate and the level of atmospheric methane $atmo_{CH_4}$ for experiments where the biosphere avoided extinction or collapse. We also find for these experiments that universally, H_2 in the ocean, $ocean_{H_2}$, was drawn down to a concentration of zero. For experiments where extinction or collapse occurred, the data points in Fig. 10 are clustered at $atmo_{CH_4} = 0$ and $ocean_{H_2} \approx 0.00042$.

Looking at the combined data we find that a large change in the burial rate, which reflects a large change in the population dynamics of our microbes, translates to a much smaller change in the abundance of methane in the atmosphere. The negative linear relationship between H_2 burial rate and atmospheric methane levels is found as the microbes growth is limited by the availability of H_2, and so microbes consume all H_2 in the ocean. This means that all hydrogen in the ocean is used in either building biomass via equation (6), or to generate ATP via equation (5). Therefore, if more H_2 is used for ATP generation, less is available for biomass production that scales linearly with biological H_2 burial rates as this is calculated by multiplying the total biomass of the biosphere by the death rate of the microbes. Note that in both equations (5) and (6) H_2O is also a product of the reactions. For every 2 moles of H_2

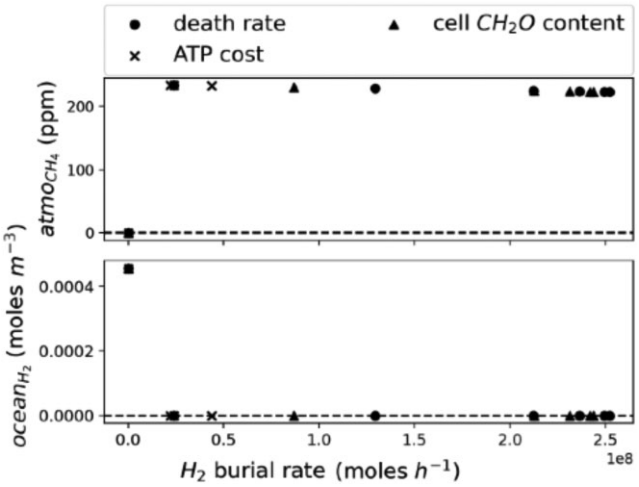

Figure 10. Top panel showing the relationship between H_2 burial rate and the level of atmospheric methane ($atmo_{CH_4}$) for all the data from changing the biological parameters. The dashed line marks $atmo_{CH_4} = 0$. Bottom panel showing the relationship between H_2 burial rate and the concentration of H_2 in the ocean ($ocean_{H_2}$) for all the data from changing the biological parameters. The dashed line marks $ocean_{H_2} = 0$.

used to create 1 mole of CH_4, an additional 2 moles of H_2 will be use to produce 2 moles of H_2O in equation (5), and for every 1 mole of H_2 converted into 1 mole of biomass (CH_2O), 1 mole of H_2 will be converted in to H_2O via equation (6).

This demonstrates that it is not necessary for a remote observer of our model planet to know the specific ATP requirements or death rates of life on the planet in order to make predictions on the level of atmospheric methane they would expect from a methane producing life form, as long as the combined biological parameters allow for a thriving biosphere on the planet. Instead, life in our model can be understood in terms of a process that convert CO_2 and H_2 to CH_4 [as in equation (5)] at a rate set by the availability of the limiting resource, in this case H_2. Therefore, we find that in order to make robust biosignature predictions, it is more important to understand the abiotic processes occurring on a planet than it is to understand the population dynamics of any alien life.

4.4 Changing the H_2 influx

In Sections 4.2.1 and 4.2.2, we showed that changing the biological parameters only had a small impact on the abundance of methane in the planet's atmosphere. Here, we demonstrate that the impact of changing the availability of H_2, the limiting resource on microbe growth, conversely has a large impact in the abundance of atmospheric methane. Fig. 11 shows the impact of changing the abiotic influx of H_2 from 0.1 times the value in Table 1 up to 5 times this value. In Fig. 11, we find that increasing the influx of H_2 corresponds to a linear increase in the microbe population and a large linear increase in the level of CH_4 in the atmosphere. The average surface temperature of the planet also significantly increases. However, the average amount of methane produced per microbe per hour, m_{CH_4}, remains constant.

Comparing Fig. 11 with Fig. 10, we see that changing the abiotic input of H_2 to the atmosphere has a much larger impact on the atmospheric methane level than changing any biological parameter. This demonstrates that, where life is limited by a resource, changing the availability of the limiting resource has a much larger impact on

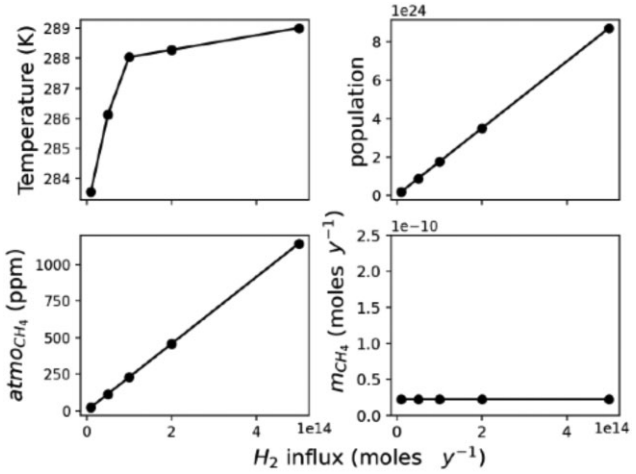

Figure 11. Panels showing the sensitivity of the surface temperature, microbe population, atmospheric CH_4 content ($atmo_{CH_4}$), and the average CH_4 output per microbe (m_{CH_4}) to changing the abiotic H_2 influx to the atmosphere.

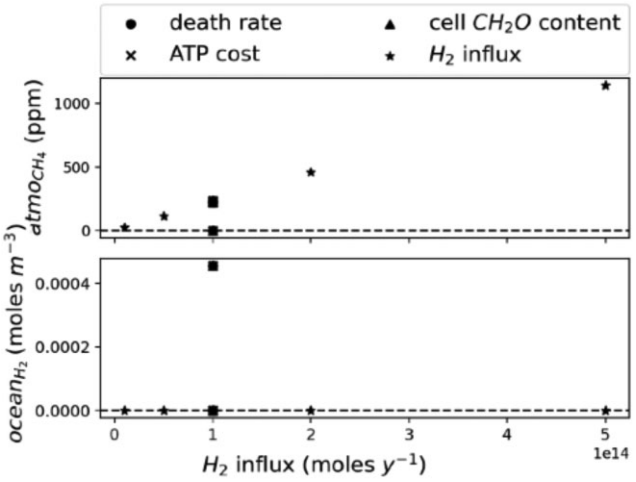

Figure 12. Figure collating all data from changing the biological parameters, and changing the H_2 influx. Top panel shows atmospheric CH_4 ($atmo_{CH_4}$) versus H_2 influx. The dashed line marks $atmo_{CH_4} = 0$. Bottom panel shows the ocean concentration of H_2 ($ocean_{H_2}$) versus H_2 influx. The dashed line marks $ocean_{H_2} = 0$.

the planet than changing biological parameters such as death rate or ATP maintenance cost.

Fig. 12 shows the data from all the experiments, both changing biological parameters and changing the H_2 influx, and shows the level of atmospheric methane against H_2 influx in the top panel, and the concentration of H_2 in the ocean against H_2 influx in the bottom panel. As we kept the H_2 influx constant for each of our biological experiments, these data points are all plotted against the same H_2 influx. The data points from the biological experiments for planets with a thriving biosphere are clustered very close together towards the lower-left part of Fig. 12, showing the small impact these parameters have on methane abundance in the atmosphere. This contrasts with the strong positive relationship seen between H_2 influx and atmospheric methane abundance. Again, experiments that resulted in extinction or only sparse life are clustered at $atmo_{CH_4} = 0$.

Looking at Fig. 12, we can clearly see that the influx of H_2, and thus the availability of the limiting resource to the biosphere, is more important for determining the level of atmospheric methane we expect as a result of our simple biosphere, than any of the parameters governing the population dynamics of the microbes. Therefore, for a remote observer of our model planet hoping to understand the amount of atmospheric methane they might expect to see in the atmosphere for a potential H_2 limited biosphere dominated by methane producing life, it would be more important for them to accurately model the H_2 influx in the atmosphere, the rate of hydrogen escape, and the breakdown of methane, rather than focusing on the population dynamics of life on the planet.

It is important to note these relationships only hold true when our model life is able to exploit hydrogen in the ocean to the same extent in each experiment. If the life became limited by some other factor in one or more of these experiments, these relationships between the biological parameters, H_2 availability and level of methane in the atmosphere would break down.

As discussed in Section 2.2, real methanogens cannot draw levels of H_2 down to zero as they are limited by diffusion. For real microbes, the limit to which they can draw down their limiting nutrient will depend on factors such as their cell size and shape, and the rate at which they require nutrients to maintain a stable population (Beveridge 1988; Koch 1996; Siefert't & Fox 1998; Schulz & Jørgensen 2001; Young 2006). We have assumed here that in each experiment the microbe have evolved to exploit H_2 to the same minimum limit, taken to be zero for simplicity. These results demonstrate that different biospheres that can exploit H_2 to the same extent, whatever the underlying population dynamics might be, will result in very similar biosignatures. Determining the limit to which life can exploit its limiting resource will be a key to understanding possible biosignatures on exoplanets.

4.5 Adding more realistic energy harvesting

We added complexity to our model by determining the amount of energy obtained from a microbe's metabolism by calculating the free energy change of the chemical reaction under the environmental conditions (see equation 7). Therefore, instead of obtaining a fixed amount of energy per mole of CH_4 produced [referred to as energy scheme (a)], the amount of energy now depends on the temperature and on the concentration of H_2, CO_2, and CH_4 in the ocean [referred to as energy scheme (b)].

Another regime is now possible in the model. When the energy obtained from a mole of H_2 remains fixed, the biosphere either exploits H_2 reserves in the ocean to zero, or collapses and goes extinct or nearly extinct. When the energy obtained per mole of H_2 is determined by equation (7), as the concentration of H_2 changes in the ocean, the energy obtained per mole of H_2 also changes. Therefore, a biosphere with a certain biological parameter setup can become limited by the energy obtained from equation (7) preventing it from drawing down the ocean concentration to zero.

Fig. 13 shows the sensitivity experiments changing the death rate of the microbes for both energy scheme (a) shown in black and (b) shown in red. The panels in Fig. 13 show how the atmospheric level of methane ($atmo_{CH_4}$), the ocean concentration of hydrogen ($ocean_{H_2}$), the microbe population, and the moles of ATP generated per mole of H_2 consumed (mol_{ATP} per mol_{H_2}) change with death rate for the two different energy schemes.

The first panel in Fig. 13 shows that for smaller death rates, the two energy schemes yield very similar levels of atmospheric methane. However, the two schemes diverge above a death rate of 15 per cent.

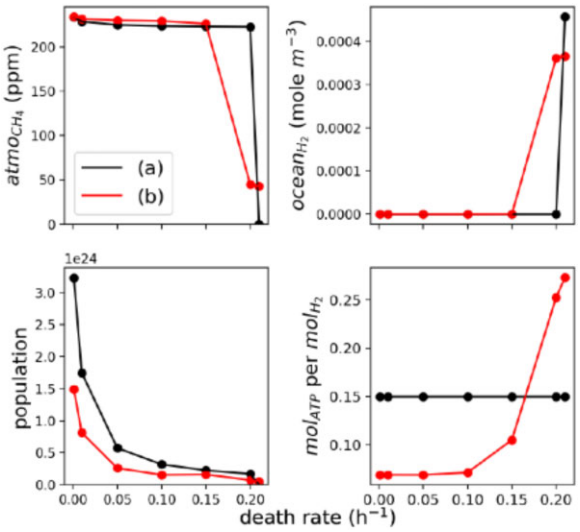

Figure 13. Panels showing the sensitivity of the atmospheric level of methane ($atmo_{CH_4}$), the ocean concentration of hydrogen ($ocean_{H_2}$), the microbe population, and the moles of ATP generated per mole of H_2 consumed (mol_{ATP} per mol_{H_2}) to changing death rate for the two different energy schemes: (a) where microbes obtain a fixed amount of energy per mole of CH_4 produced, and (b) where this energy is given by the free energy change of $CO_2 + 4H_2 \rightarrow CH_4 + 2H_2O$ – the microbes' metabolism.

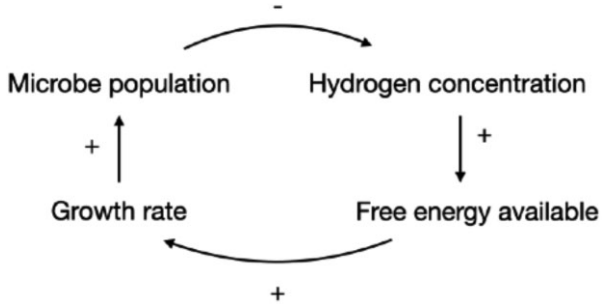

Figure 14. Diagram showing the feedback loop between the H_2 ocean concentration, free energy available, growth rate of the microbes and the total population of the biosphere. A + sign indicates than an increase in the source leads to an increase in the sink. A − sign indicates that an increase in the source leads to a decrease in the sink.

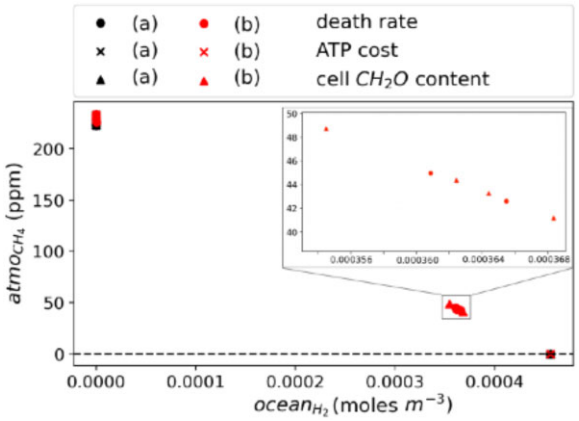

Figure 15. Atmospheric methane abundance ($atmo_{CH_4}$) versus ocean H_2 content ($ocean_{H_2}$) for experiments changing biological parameters of death rate, ATP maintenance cost, and protein cell content for experiments where (a) microbes obtain a fixed amount of energy per mole of CH_4 produced, and (b) where this energy is given by the free energy change of $CO_2 + 4H_2 \rightarrow CH_4 + 2H_2O$ – the microbes' metabolism. The dashed line marks $atmo_{CH_4} = 0$.

For a death rate of 20 per cent, the biosphere under energy scheme (a) is H_2 limited and produces a similar level of atmospheric methane as biospheres with smaller death rates. The biosphere with a death rate of 20 per cent under energy scheme (b), however, does not draw the level of H_2 in the ocean to zero. Instead, the H_2 concentration in the ocean remains higher, and the corresponding level of atmospheric methane is greatly reduced. With a high death rate, microbes must reproduce faster to maintain a stable population. When the energy obtained per mole of H_2 is fixed, the microbe is limited only by hydrogen availability and $C^{H_2}_{max}$ – the maximum rate at which it can consume H_2. However, when the energy obtained per mole of H_2 is determined by equation (13), the energy obtained per mole of H_2 consumed will change as the concentration of H_2 in the ocean changes. Therefore, microbes will be able to draw the level of hydrogen down in the ocean to the level where they obtain sufficient energy from $C^{H_2}_{max}$ moles of H_2 to maintain a stable population.

A slightly different feedback loop comes into effect when the microbe biosphere is limited by the energy yield of equation (7). Now the free energy available plays a role in determining the microbe population the planet can support for any biological parameter combination that pushes the system out of the purely H_2 availability limited regime e.g. a high death rate of 20 per cent as shown in Fig. 13. Fig. 14 shows the stabilizing feedback loop between the H_2 ocean concentration, free energy available, growth rate of the microbes, and the total population of the biosphere.

We repeated the previous experiments of changing the biological parameters while utilizing energy scheme (b). Fig. 15 shows the abundance of atmospheric methane against the ocean concentration of H_2 for all the biological experiments from Sections 4.2.1 and 4.2.2, labelled (a) and shown in black, combined with results from repeating these experiments but with realistic energetics from equation (7), labelled (b) and shown in red. We see three clear groupings of data points in Fig. 15 – a cluster of points for an ocean concentration of H_2, where the corresponding levels of atmospheric CH_4 – $atmo_{CH_4}$, are clustered around roughly $atmo_{CH_4} = 220$. This is the regime where the biosphere is able to exploit all the H_2 in the ocean and is solely limited in growth by the availability of H_2. The total populations of the different biospheres in these cases leads to only slight changes in the abundance of atmospheric methane.

Another cluster of points are seen in Fig. 15 between $ocean_{H_2} = 0.003$ and $ocean_{H_2} = 0.004$. Here, we find only data points from experiments under energy scheme (b) and this is the regime where the biosphere is limited by the free energy available from equation (7). For biospheres requiring more energy to maintain a stable population, a higher concentration of H_2 in the ocean is necessary, as per the feedback loop in Fig. 14. In this cluster of data points, an inverse linear relationship exists between $atmo_{CH_4}$ and $ocean_{H_2}$ – as the level of H_2 in the ocean increases, the level of methane in the atmosphere decreases linearly. Therefore, determining the extent to which a biosphere can exploit H_2 in the ocean determines the biosignature.

Fig. 15 shows a third cluster of data points where $atmo_{CH_4} = 0$. These are experiments where life went extinct and so no biosignature is present on the planet. Fig. 15 shows a clear relationship between H_2 availability in the ocean and CH_4 levels in the atmosphere for all experiments.

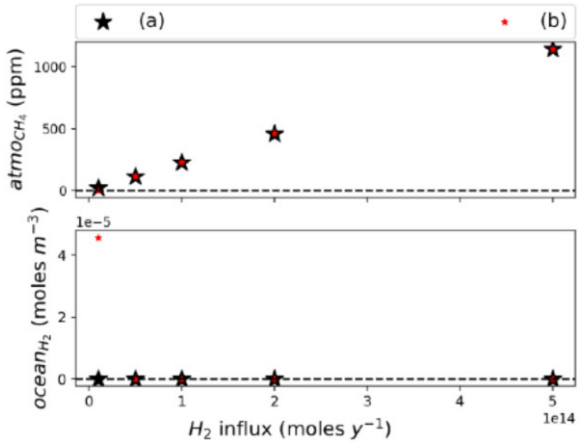

Figure 16. Atmospheric methane abundance ($atmo_{CH_4}$), and ocean concentration of H_2 ($ocean_{H_2}$) versus H_2 influx for experiments changing the H_2 influx for two scenarios where (a) microbes obtain a fixed amount of energy per mole of CH_4 produced, and (b) where this energy is given by the free energy change of $CO_2 + 4H_2 \rightarrow CH_4 + 2H_2O$ – the microbes metabolism. The dashed lines mark $atmo_{CH_4} = 0$ and $ocean_{H_2} = 0$ in the top and bottom panels, respectively.

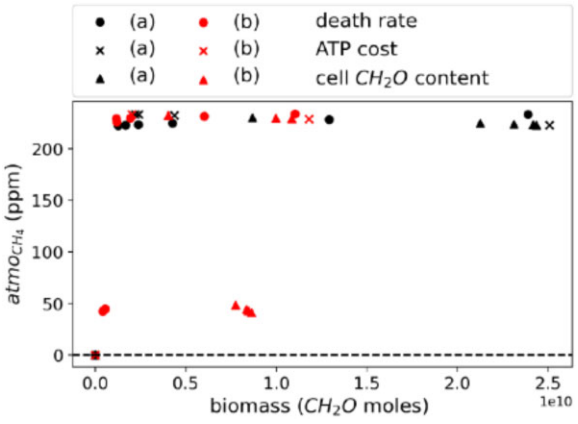

Figure 17. Atmospheric methane abundance ($atmo_{CH_4}$) versus biomass (moles of CH_2O contained within the biosphere) for experiments changing biological parameters of death rate, ATP maintenance cost, and protein cell content for experiments, where (a) microbes obtain a fixed amount of energy per mole of CH_4 produced, and (b) where this energy is given by the free energy change of $CO_2 + 4H_2 \rightarrow CH_4 + 2H_2O$ – the microbes' metabolism. The dashed line marks $atmo_{CH_4} = 0$.

Fig. 16 shows the data for changing H_2 influx versus methane content when adopting energy scheme (b; shown in red), and the corresponding results from the previous experiments (from Section 4.4) where energy scheme (a) was used (shown in black). We find again that changing the H_2 influx has a significant impact of the level of methane in the atmosphere and these data points very closely overlap. We see a very slight difference between the two energy schemes in the data points for the lowest H_2 influx, but in this case, in the experiment using energy type (b) life went extinct on the planet resulting in no atmospheric methane.

Our model setup has included only one species of life and so there is no inter-species competition for resources. Where the biosphere is able to exploit all the H_2 in the ocean, the exact details of the microbes, e.g. death rate or ATP maintenance cost, have only a minimal impact on the abundance of atmospheric CH_4. For two species with differing biological parameters but the same ability to exploit H_2 in the ocean, neither will have a selective advantage over the other, and the methane biosignature is only minimally impacted by whichever species becomes dominant. For situations where the biosphere becomes limited by the free energy available from equation (7), these parameters can now have an impact on the limit to which the biosphere can draw H_2 down in the ocean, and this will then impact the resulting abundance of atmospheric methane. However, in a scenario with multiple species, the species capable of drawing H_2 down to the lowest concentration in the ocean would have the selective advantage as its growth rate will not become limited as quickly as other species as the H_2 concentration in the ocean drops. Therefore, we would expect the species that can draw down ocean H_2 to the lowest concentration to out-compete other species (Tilman 2020). Determining the methane biosignature for a nutrient-limited biosphere would therefore depend on determining the theoretical limit to which life can evolve to exploit the limiting nutrient.

4.6 Biomass as a metric for predicting the methane biosignature

Methods of predicting potential biosignatures include a biomass-based model to estimate the plausibility of exoplanet biosignature gases developed by Seager et al. (2013a). In this biomass-based model, potential biosignatures are calculated based on Earth-based measurements of maximum biomass per area, and maximum gas output rates for different species. Seager et al. (2013a) combine this data to obtain a theoretical maximum biosignature strength to be used to verify future possible biosignature observations. The biomass-based model determines whether the abundance of a proposed biosignature gas in the atmosphere of an exoplanet would be biologically viable to be the product of life. The work in this paper presents a different approach for predicting biosignatures by instead focusing on determining the possible limiting factors on a biospheres growth to constrain possible biosignatures. In this approach, it then becomes crucial to understand the availability of the limiting resource, which in the case of an H_2 limited biosphere as considered in this work, will depend on factors such as the level of volcanic activity and the rate of H_2 loss to space.

Fig. 17 shows the data from our experiments in changing the biological parameters for both energy schemes (Sections 4.2.1 and 4.2.2) and shows how the level of atmospheric methane $atmo_{CH_4}$ changes with the biomass of the biosphere. The biomass is calculated in terms of number of moles of CH_2O contained within the living microbe cells. The three regimes: H_2 availability limited, energetically limited, and biosphere collapse/extinction are clearly seen in Fig. 17 separated along the y-axis, however, no clear relationship emerges between biomass and $atmo_{CH_4}$. Fig. 17 shows that large variations in biomass can result in very similar levels of CH_4 and so in the case of a nutrient-limited biosphere biomass would be a poorer metric for predicting a possible type I biosignature than determining the limiting nutrient of the biosphere and the biosphere's ability to exploit this nutrient.

5 SUMMARY

We have shown that for a simple single-species H_2-limited biosphere, the underlying population dynamics of the microbes are largely irrelevant to the abundance of atmospheric methane in the atmosphere – taken in these experiments as our biosignature – instead the limit to which the biosphere can exploit H_2 in the ocean is more fundamental.

While different biospheres might have different total populations, if two differing biospheres are capable of drawing down ocean concentrations of H_2 to the same limit, their relative population dynamics only minimally impact the resulting biosignature. We found that the influx of H_2 to the atmosphere of the planet had a far stronger impact on the level of CH_4 in the atmosphere. Understanding the abiotic processes governing the availability of the limiting resource to the biosphere, in this case H_2, and the biosignature gas, CH_4, are crucial for biosignature predictions for nutrient-limited biospheres. The highly simplified abiotic environment of our model planet allows the impact on the atmospheric composition due to the population dynamics of the biosphere to be clearly determined; however, for forming biosignature predictions for real planets, a far more sophisticated representation of the abiotic environment will be necessary.

We have considered a type I biosignature in this model as classified in Seager et al. (2013a) where the biosignature is generated as a by-product from microbial energy extraction and the results from this work are only applicable to forming predictions for biosignatures of this type. Biosignatures resulting from processes other than energy extraction of microbes might behave differently with the biological parameters explored in this work.

We found that adding complexity to this model in the form of an accurate representation of the energy obtained from the microbes' metabolisms based on the change of free energy of converting H_2 and CO_2 to CH_4 and H_2O does not change these results while the biosphere draws H_2 in the ocean to zero. As the microbe parameters are increased to the limit where a biosphere with energy scheme (a) would goes extinct, an energetically limited regime emerges, where a viable biosphere is still possible but now only for higher concentrations of H_2 in the ocean. As the energy obtained per moles of H_2 consumes depends on the ocean concentrations of CO_2, H_2, and CH_4 under energy scheme (b), a more gradual decline in the biosignature occurs, where the level of CH_4 in the atmosphere decreases linearly as the concentration of H_2 increases in the ocean. In this work, we have modelled biospheres consisting of only a single species of microbe and so inter-species competition is not present. However, if multiple species limited by H_2 coexisted, the species capable of drawing H_2 down to the lowest concentration would have the selective advantage and compete the others (Tilman 2020). Therefore, inter-species competition would lead to limiting nutrients being drawn down to the lowest limit possible. Determining this lowest possible limit for each potential limiting nutrient will be a key for making biosignature predictions using this method.

These results help deepen our understanding of life–planet interactions. It reduces the need to make unnecessary assumptions about alien life based on life on Earth. These results show that when considering a nutrient-limited biosphere it is more important to accurately model the processes that regulate the availability of the limiting nutrient, and determine the limit to which life can exploit this nutrient, than it is to model any specific population dynamics for that biosphere. In our model example, these key processes are: the influx of H_2 to the atmosphere, the rate of H_2 loss to space, and the rate of methane breakdown back to H_2 and CO_2. Changing the rate of any of these processes will have a much stronger impact on the abundance of methane we expect to find in the atmosphere of our model planet than changing any parameter dealing with the population dynamics of the microbes. This understanding is already used in studies of Earth history to recreate past climates (Herman & Kump 2005; Kharecha et al. 2005; Bruggeman & Bolding 2014; Lenton et al. 2018; Zakem et al. 2020), and the work in this study is supported by models of Earth's biosphere.

Identifying possible metabolic pathways will of course be key to understanding potential biosignatures, as we will need to know what by-products we expect from various types of life on any potentially inhabited planet. Quantifying the free energy available to a biosphere will also be important, as will estimating recycling efficiency once multiple types of life are involved. However, understanding detailed population dynamics of a potential alien biosphere will not be necessary for us to predict potential type I biosignatures for nutrient-limited biospheres. Given that we cannot go and measure any potential alien biology in a lab, and that our understanding of life is inherently biased towards Earth-based life, this significantly reduces the number of assumptions needed to accurately model a proposed alien biosphere under nutrient limitation, and helps us avoid biases based on our understanding of specific organisms on Earth.

This method for predicting possible type I biosignatures depends on understanding the abiotic sources of nutrients available to a biosphere. However, remote detection of, for example, levels of volcanic activity are unfeasible, and predicting these factors for any planet will depend on modelling and further developing our understanding of planet formation. As so many unknowns exist and will continue to exist for any potential future biosignature detections, multiple methods for biosignature verification are required to increase confidence that a potential biosignature is actually due to life. We hope that this work provides an additional tool to the astrobiology community to help verify any possible future biosignature detections.

6 NEXT STEPS

The results presented here are highly simplified to enable us to pull out clear relationships between various parameters and the strength of life's impact on its host planet when limited by nutrient availability. We have only considered a planet with a single life form, however, any life-bearing exoplanet is more likely to have a diverse biosphere. A diversity of metabolisms are deeply rooted in the 'tree' of life on Earth, and the earliest fossil evidence for life on Earth is of five morphologically distinct species of microbe, indicating that diversification happened quickly (Schopf et al. 2018). Therefore, exploring more complex biospheres will be a necessary step in increasing the applicability of this approach to potentially inhabited exoplanets. Additionally, abstract models of ecology predict that higher diversity ecosystems will on average persist for longer than low diversity ecosystems (Christensen et al. 2002; Arthur & Nicholson 2022). This would make it statistically more likely to observe biosignatures produced by complex ecosystems rather than simple ones increasing the importance of modelling these scenarios.

The results in this paper only hold true where our microbe life is limited by a chemical resource, in this case H_2. When this is no longer true and some other factor is limiting the biosphere, this new limiting factor will then become the key parameter to understanding how potential biosignatures might manifest on a planet. The atmospheric chemistry in our model was kept very simple and for future work we intend to move away from this simple framework to more sophisticated models of atmospheric chemistry and more realistic models of biogeochemistry, adapted from modelling Earth's history (Daines, Mills & Lenton 2017; Lenton et al. 2018). These results show that when considering a nutrient-limited life-form, we can reduce the bulk of the impact on its host planet down to its metabolism, and the availability of the limiting nutrient. This study takes a step towards allowing us to insert a very simple biological framework into more sophisticated climate models to achieve robust predictions on possible biosignatures. As discussed, determining the

limit to which any life-form can exploit its limiting nutrient will be a key for accurate biosignatures predictions.

Of course not all life is nutrient limited, on Earth much of our biosphere is photon limited, and in future work, we aim to recreate the experiments demonstrated here but for a photon limited life-form to determine the minimal assumptions needed about life existing under those circumstances. This would allow us to model both life limited by nutrients, and by photon availability in a simple robust manner, allowing us to form hypotheses for potential biosignatures for either case.

We also hope to use this understanding to consider possible biosignatures on 'Super Earths' – planets that have a radius of 1.25–2 times that of Earth's Fressin et al. (2013). Super Earths are some of the most commonly found planets with current observational limitations that make them interesting candidates in the search for biosignatures. Some of these planets are theorized to have atmospheres far richer in hydrogen than Earth's due to less hydrogen loss to space (Seager, Bains & Hu 2013b). Our test model set-up above explores scenarios where life is limited by hydrogen. On a hydrogen-rich super Earth, this may no longer be the case. A high concentration of H_2 could become an important greenhouse gas (Pierrehumbert & Gaidos 2011), providing significant warming to the planet (which is not the case on Earth). How life would balance the requirement of atmospheric H_2 to keep its planet warm against its need to consume H_2 would be a key for understanding the potential biosignatures that might be possible on such a planet. The temperature dependence of microbe' metabolisms [as the temperature decreases metabolic activity tends to decrease (Clarke & Fraser 2004)] could become an important factor to consider when predicting possible biosignatures on such planets.

We have focused on methanogens, but can easily incorporate different metabolisms, or scenarios with multiple competing metabolisms. This work represents the first step in trying to frame our understanding of how a relatively arbitrary life-form may interact with its planetary atmosphere, and to determine the key parameters or factors necessary to explore and characterize this interaction. It is clear that there is much work to do, requiring a large and diverse community, to enable us to be in a position to confidently, and robustly, determine the presence of a biosignature in addition to developing more sensitive and accurate instrumentation.

ACKNOWLEDGEMENTS

We would like to thank the reviewer for their helpful feedback on earlier drafts of this paper. Material produced using Met Office Software. We acknowledge use of the Monsoon2 system, a collaborative facility supplied under the Joint Weather and Climate Research Programme, a strategic partnership between the Met Office and the Natural Environment Research Council. This work was supported by a Leverhulme Trust research project grant [RPG-2020-82], a Science and Technology Facilities Council Consolidated Grant [ST/R000395/1], a UK Research and Innovation Future Leaders Fellowship [MR/T040866/1], and a John Templeton Foundation grant. Eager-Nash would like to thank the Hill Family Scholarship, generously supported by University of Exeter alumnus, and president of the University's US Foundation Graham Hill (Economic & Political Development, 1992) and other donors to the US Foundation.

DATA AVAILABILITY STATEMENT

The code used to generated the data in this study can be found at: https://github.com/nicholsonae/archean_world

REFERENCES

Alcabes O. D., Olson S., Abbot D. S., 2020, MNRAS, 492, 2572
Arthur R., Nicholson A., 2022, J. Theor. Biol., 533, 110940
Beveridge T., 1988, Can. J. Microbiol., 34, 363
Boutle I. A., Mayne N. J., Drummond B., Manners J., Goyal J., Lambert H. F., Acreman D. M., Earnshaw P. D., 2017, A&A, 601, 13
Brady P. V., Carroll S. A., 1994, Geochim. Cosmochim. Acta, 58, 1853
Brown J. H., Gillooly J. F., Allen A. P., Savage V. M., West G. B., 2004, Ecology, 85, 1771
Bruggeman J., Bolding K., 2014, Environ. Modelling Softw., 61, 249
Catling D. C. et al., 2018, Astrobiology, 18, 709
Catling D. C., Zahnle K. J., 2020a, Sci. Adv., 6, eaax1420
Catling D. C., Zahnle K. J., 2020b, Sci. Adv., 6, eaax1420
Catling D. C., Zahnle K. J., McKay C. P., 2001, Science, 293, 839
Cermak N., Becker J. W., Knudsen S. M., Chisholm S. W., Manalis S. R., Polz M. F., 2017, ISME J., 11, 825
Christensen K., Di Collobiano S., Hall M., Jensen H. J., 2002, J. Theor. Biol., 216, 73
Clarke A., Fraser K., 2004, Funct. Ecol., 18, 243
Claudi R., 2017, preprint (arXiv:1708.05829)
Daines S. J., Mills B. J., Lenton T. M., 2017, Nature Commun., 8, 1
Eager J. K. et al., 2020, A&A, 639, A99
Fressin F. et al., 2013, ApJ, 766, 81
Fujii Y. et al., 2018, Astrobiology, 18, 739
Grimm V., Railsback S. F., 2013, Individual-based Modeling and Ecology. Princeton Univ. Press, Princeton, NJ
Hellweger F. L., Bucci V., 2009, Ecol. Modelling, 220, 8
Herman E., Kump L., 2005, Geobiology, 3, 77
Hunten D., 1973, J. Atmos. Sci., 30, 1481
Janssen P. H., Schuhmann A., Bak F., Liesack W., 1996, Arch. Microbiol., 166, 184
Kasting J. F., 2005, Precambrian Res., 137, 119
Kasting J., Zahnle K., Walker J., 1983, Precambrian Res., 20, 121
Kharecha P., Kasting J., Siefert J., 2005, Geobiology, 3, 53
Kiang N. Y., Domagal-Goldman S., Parenteau M. N., Catling D. C., Fujii Y., Meadow V. S., Schwieterman E. W., Walker S. I., 2018, Astrobiology, 18, 619
Koch A. L., 1996, Annu. Rev. Microbiol., 50, 317
Kral T. A., Brink K. M., Miller S. L., McKay C. P., 1998, Orig. Life Evol. Biosph., 28, 311
Krissansen-Totton J., Thompson M., Galloway M. L., Fortney J. J., 2022, Nature Astronomy, 6, 189
Lennon J., Jones S., 2011, Nature Rev. Microbiol., 9, 119
Lenton T. M., Daines S. J., Mills B. J. W., 2018, Earth Sci. Rev., 178, 1
Li J. et al., 2019, ISME J., 13, 2162
Liss P., Slater P., 1974, Nature, 247, 181
Lovelock J. E., Margulis L., 1974, Tellus, 26, 1
Lynch T., Wanga Y., van Brunta B., Pachecob D., Janssenb P., 2019, J. Theor. Biol., 477, 14
Lyu Z., Shao N., Akinyemi T., Whitman W. B., 2018, Curr. Biol., 28, R727
Margulis L., Lovelock J., 1974, Icarus, 21, 471
Meadows V. S. et al., 2018, Astrobiology, 18, 630
Monod J., 1949, Annual review of microbiology, 3, 371
Nicholson A. E., Wilkinson D. M., Williams H. T. P., Lenton T. M., 2018b, MNRAS, 477, 727
Nicholson A. E., Wilkinson D. M., Williams H. T., Lenton T. M., 2017, J. Theor. Biol., 414, 17
Nicholson A. E., Wilkinson D. M., Williams H. T., Lenton T. M., 2018a, J. Theor. Biol., 457, 249
Nisbet E. G., Sleep N. H., 2001, Nature, 409, 1083
Pierrehumbert R., Gaidos E., 2011, ApJ, 734, L13
Quanz S. P. et al., 2021, Exp. Astron., 10, 1
Schopf J. W., Kitajima K., Spicuzza M. J., Kudryavtsev A. B., Valley J. W., 2018, Proc. Natl. Acad. Sci., 115, 53
Schulz H. N., Jørgensen B. B., 2001, Annu. Rev. Microbiol., 55, 105
Schwieterman E. W. et al., 2018, Astrobiology, 18, 663
Seager S., 2013, Science, 340, 577

Seager S., Bains W., Hu R., 2013a, ApJ, 775, 104
Seager S., Bains W., Hu R., 2013b, ApJ, 777, 95
Şengör S. S., Ginn T. R., Brugato C. J., Gikas P., 2013, Biochem. Eng. J., 81, 65
Siefert't J. L., Fox G. E., 1998, Microbiology, 144, 2803
Snellen I. A. G. et al., 2021, Exp. Astron., 15, 1
Tilman D., 2020, in Resource Competition and Community Structure.(MPB-17), Vol. 17. Princeton Univ. Press, Princeton
Walker J., 1977, Evolution of the Atmosphere. New York: Macmillan, New York
Walters D. et al., 2019, Geosci. Model Dev., 12, 1909
Wang Y., Janssen P. H., Lynch T. A., van Brunt B., Pacheco D., 2016, J. Theor. Biol., 393, 75
Weissman J. L., Hou S., Fuhrman J. A., 2021, Proc. Natl. Acad. Sci., 118, e2016810118
Wilkinson D. M., 2007, Fundamental Processes in Ecology: An Earth Systems Approach. OUP Oxford, Oxford, UK
Williams H. T., Lenton T. M., 2007, Oikos, 116, 1087
Woese C. R., Fox G. E., 1977, Proc. Natl. Acad. Sci., 74, 5088
Young K. D., 2006, Microbiol. Mol. Biol. Rev., 70, 660
Zahnle K. J., 1986, J. Geophys. Res.: Atmospheres, 91, 2819
Zakem E. J., Polz M. F., Follows M. J., 2020, Nature Commun., 11, 1
Zhang Y., Chen Y., Zhan T., Zheng Y., Zheng X., He M., 2018, Fluid Phase Equilib., 474, 126

This paper has been typeset from a TEX/LATEX file prepared by the author.